Geol. Mag. **148** (*4*), *2011, pp. 511–528. © Cambridge University Press 2011*
doi:10.1017/S001675681100001X

Strontium-, carbon- and oxygen-isotope compositions of marbles from the Cycladic blueschist belt, Greece

CLAUDIA GÄRTNER*†‡, MICHAEL BRÖCKER*, HARALD STRAUSS‡ &KATJA FARBER*

*Institut für Mineralogie, Universität Münster, Corrensstr. 24, 48149 Münster, Germany
‡Institut für Geologie und Paläontologie, Universität Münster, Corrensstr. 24, 48149 Münster, Germany

(*Received* 20 November 2009; *accepted* 1 November 2010; *first published online* 3 February 2011)

Abstract – The Cycladic blueschist belt, Greece, is mostly submerged below sea level and regional correlations are difficult to establish. Marbles are widespread within the belt and locally used as marker horizons to subdivide monotonous schist sequences. However, owing to the lack of distinctive petrographic characteristics, the marbles have not been used for island-to-island correlations. This study aims to investigate the potential of Sr-, C- and O-isotope compositions of marbles as a tool for unravelling the litho- and/or tectonostratigraphic relationships across the Cycladic islands, and as a proxy for the time of sediment formation. For this purpose, we have studied metamorphic carbonate rocks from the islands of Tinos, Andros, Syros, Sifnos and Naxos. Identical $^{87}Sr/^{86}Sr$ values for certain marble horizons occurring on Tinos, Andros and Sifnos are interpreted to document coeval regional carbonate precipitation. The $^{87}Sr/^{86}Sr$ values of the apparently least altered samples intersect the seawater curve multiple times within the most likely time interval of original carbonate precipitation (< 240 Ma; as indicated by previously published ion probe U–Pb zircon data) and thus an unequivocal age assignment is not possible. Very broad temporal correlations are possible, but more subtle distinctions are not feasible. On Andros, the overlapping Sr-isotope values of marbles representing the lowest and highest parts of the metamorphic succession are in accordance with a model suggesting isoclinal folding or thrusting of a single horizon, or very fast sedimentation. In contrast, distinct $^{87}Sr/^{86}Sr$ values for samples from Tinos, representing different levels of the metamorphic succession, suggest that these rocks represent a temporal succession and not the tectonic repetition of a single horizon. Based on Sr-, O- and C-isotope characteristics alone the time equivalence of marbles occurring on different islands could not be documented unambiguously. However, by using various combinations of these parameters, some occurrences can be discriminated from the overall sample population. The new data further accentuate the general potential of coupled Sr-, C- and O-isotope characteristics for identification of archaeological provenance and complement existing datasets for Aegean marbles.

Keywords: Sr isotopes, C and O isotopes, marble, Cycladic blueschist belt, Greece.

1. Introduction

The Attic–Cycladic crystalline belt in the central Aegean region (Fig. 1a) is a major tectonostratigraphic unit of the Hellenides. Known outcrops roughly delineate an area of *c*. 30 000 km^2, but most parts of this terrane are submerged below sea level. The Attic–Cycladic crystalline belt records a complex structural and metamorphic evolution which documents various stages in the closure of the Neotethys Ocean and the extensional collapse of the newly formed orogen (e.g. Jolivet & Patriat, 1999; Krijgsman, 2002; Jolivet *et al*. 2003). Regional correlations between different islands are difficult to establish owing to the lack of distinct marker horizons and incomplete knowledge of protolith ages for most parts of the metamorphic succession. The general geological and metamorphic framework is well-documented, but key information pertaining to the pre-metamorphic evolution and the tectonostratigraphy is only poorly constrained.

†Author for correspondence: c_gaer01@uni-muenster.de

This study aims at utilizing strontium-, carbon- and oxygen-isotope compositions recorded in marbles as a tool for unravelling litho- and/or tectonostratigraphic relationships across the northern part of the Cyclades as well as the time of sediment deposition. On a local scale, marbles are used as marker horizons to subdivide monotonous schist sequences (e.g. Tinos and Andros; Melidonis, 1980; Papanikolaou, 1978*a*,*b*), but petrographic characteristics alone are not sufficient to establish correlations between distinct marble horizons occurring on different islands. Sr-, C- and O-isotope data may help to unravel such relationships.

Besides documentation of isotope geochemical affinities between different marble occurrences, valuable information about the time of sediment formation may be obtained. Owing to its long residence time, seawater records a global $^{87}Sr/^{86}Sr$ isotope signature that is controlled by variable Sr contributions from terrestrial weathering and hydrothermal alteration of basalts (e.g. Banner, 2004 and references therein). A well-established Sr-isotope record for Phanerozoic seawater (e.g. Veizer *et al*. 1999; McArthur, Howarth & Bailey, 2001) can be used as a reference for

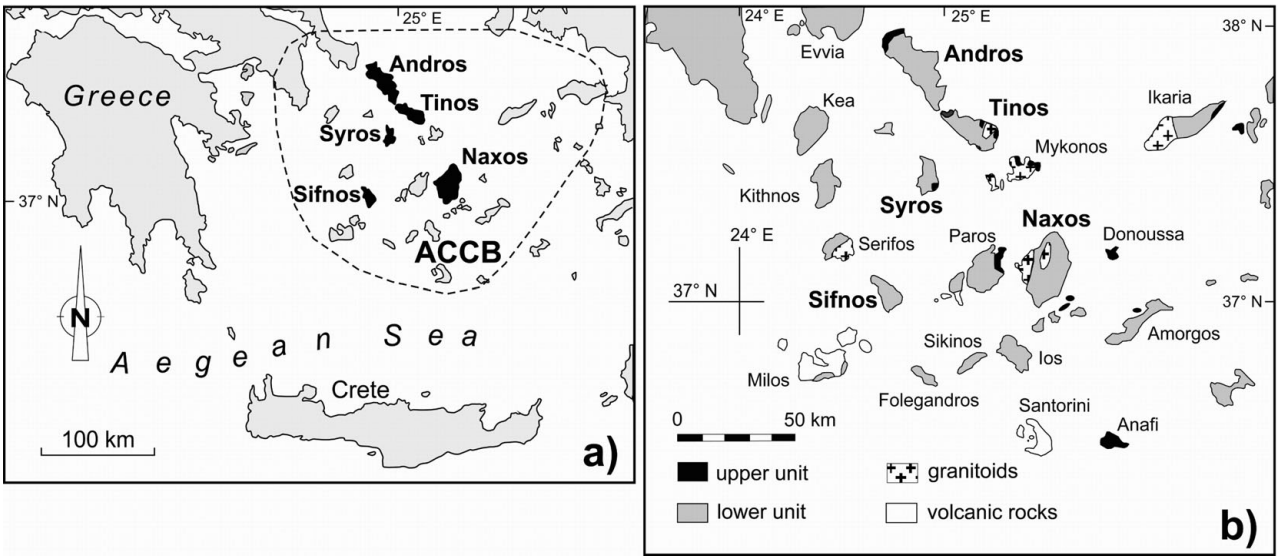

Figure 1. Simplified geological overview of the Aegean region (modified after Matthews & Schliestedt, 1984) with key locations discussed in the text. ACCB – Attic–Cycladic crystalline belt.

Sr-isotope chemostratigraphy of marine carbonates. The Sr-isotope composition is very susceptible to diagenetic and metamorphic alteration, which may obscure the original composition (e.g. McArthur, 1994; Banner, 2004; van Geldern *et al*. 2006; Nascimento, Sial & Pimentel, 2007). The Cycladic marbles have experienced diagenesis and at least two stages of tectonometamorphic overprinting at eclogite to blueschist facies and greenschist to amphibolite facies *P–T* conditions, respectively. It is, thus, uncertain whether or not this material is suitable for a chemostratigraphic study using Sr isotopes. However, previous studies have documented that high-grade metamorphic carbonate rocks can retain their original Sr-, C- and/or O-isotopic signatures under favourable circumstances (Melezhik *et al*. 2001, 2005; Thomas *et al*. 2004). We studied selected marble occurrences from the islands of Tinos, Andros, Syros, Sifnos and Naxos (Fig. 1a, b), which represent key locations for the tectonometamorphic evolution of the Cyclades. Here, we report field observations, petrographic characteristics and results of various geochemical analyses (Sr, C, O isotopes; selected trace elements).

2. Regional geology

The Attic–Cycladic crystalline belt consists of two major structural units that are separated by low-angle normal faults (e.g. Dürr *et al*. 1978; Okrusch & Bröcker, 1990; Avigad *et al*. 1997). The upper unit is poorly exposed (Fig. 1b) and comprises a heterogeneous sequence of unmetamorphosed Permian to Neogene sediments, ophiolites, greenschist-facies rocks with Cretaceous to Tertiary metamorphic ages (Bröcker & Franz, 1998, 2006), as well as Late Cretaceous granitoids and medium-pressure/high-temperature metamorphic rocks (e.g. Patzak, Okrusch & Kreuzer, 1994 and references therein). The lower unit (hereafter referred to as the Cycladic blueschist unit) comprises a pre-Alpine crystalline basement and a metamorphosed volcano-sedimentary succession (e.g. Dürr *et al*. 1978; Okrusch & Bröcker, 1990). Both experienced at least two stages of metamorphism in Tertiary times. During the first stage, eclogite to epidote–blueschist-facies conditions were reached ($T = \sim 450$–$550\,^{\circ}C$, $P = \sim 12$–20 kbar; e.g. Bröcker *et al*. 1993; Trotet, Jolivet & Vidal, 2001). In the northern and central Cyclades, subsequent overprinting occurred at greenschist-facies conditions ($T = \sim 450$–$550\,^{\circ}C$, $P = \sim 4$–9 kbar; e.g. Bröcker *et al*. 1993; Parra, Vidal & Jolivet, 2002), whereas the southern Cyclades (e.g. Naxos) experienced amphibolite-facies metamorphism and partial melting (e.g. Buick & Holland, 1989). Regional metamorphism was followed by widespread intrusion of granitoids (e.g. Altherr & Siebel, 2002). High-pressure (HP) rocks mostly yield Eocene (55–40 Ma) metamorphic ages, while ages for greenschist- to amphibolite-facies rocks cluster in the Late Oligocene and Miocene (*c*. 25–16 Ma; e.g. Altherr *et al*. 1979, 1982; Wijbrans & McDougall, 1988; Wijbrans, Schliestedt & York, 1990; Bröcker *et al*. 1993, 2004; Bröcker & Franz, 1998, 2006). HP metamorphism is mostly considered to be restricted to the Eocene (e.g. Tomaschek *et al*. 2003), but may have started as early as Cretaceous time (*c*. 80 Ma; Bröcker & Enders, 1999, 2001; Bröcker & Keasling, 2006).

3. Local geology

On Tinos, a representative fragment of the Attic–Cycladic crystalline belt is exposed in at least three tectonic subunits (Fig. A1 in online Appendix at http://journals.cambridge.org/geo). The two tectonic subunits occupying the highest structural levels (Akrotiri Unit and Upper Unit) belong to the upper main unit of the Attic–Cycladic crystalline belt and record amphibolite- and/or greenschist-facies *P–T* conditions

https://doi.org/10.1017/S001675681100001X Published online by Cambridge University Press

(e.g. Patzak, Okrusch & Kreuzer, 1994; Katzir *et al*. 1996; Bröcker & Franz, 1998). Most of the island is a part of the Cycladic blueschist unit, which is represented by a coherent marble–schist sequence (= Lower Unit; about 1250 m to 1800 m in thickness). Variably rounded meta-ophiolitic blocks and rock fragments of all sizes (mostly < 1 to 10 m, but up to 300 m) occur widely scattered throughout the Lower Unit (Bulle *et al*. 2010). Although remnants of HP rocks are locally preserved, pervasively overprinted rocks with greenschist-facies mineral assemblages are more common (e.g. Melidonis, 1980; Bröcker *et al*. 1993). The whole succession can be subdivided by means of three mappable marble horizons, m3, m2 and m1 (Melidonis, 1980; Fig. A3 in online Appendix at http://journals.cambridge.org/geo). Phengite-bearing marbles of these horizons were used for Rb–Sr and Ar–Ar white mica geochronology, indicating metamorphic ages ranging between 43 and 24 Ma (Bröcker *et al*. 2004; Bröcker & Franz, 2005). The lowermost part of the metamorphic rock pile, which consists of dolomite marbles and minor phyllites, has been interpreted as a para-authochthonous Basal Unit (Avigad & Garfunkel, 1989). Other studies considered the basal carbonate sequence as an integral part of the Lower Unit (Melidonis, 1980; Bröcker & Franz, 2005) and related a tectonic contact on top of this sequence to post-orogenic extension (Gautier & Brun, 1994; Bröcker & Franz, 2005). From the dolomites, Melidonis (1980) reported findings of Upper Triassic marine fossils. No biostratigraphic remnants are preserved in the calcite marbles occurring at higher lithostratigraphic levels. The depositional age of the metasedimentary sequences has been inferred to be Triassic to Jurassic, but recent U–Pb dating of zircons from siliciclastic rocks documented a Cretaceous age group (*c*. 80 Ma) that suggests a considerably younger maximum depositional age (C. Gärtner, unpub. M.Sc. thesis, Univ. Münster, 2008; Bulle *et al*. 2010). The Cretaceous ages in metasediments perfectly correlate with U–Pb zircon ages of meta-igneous blocks, lending support to interpretations suggesting an olistostromatic origin for the Cycladic mélange sequences (Bulle *et al*. 2010). In eastern Tinos (Fig. A1), a composite Miocene granitoid intrusion (*c*. 17–14 Ma; Altherr *et al*. 1982; Bröcker & Franz, 1998) caused contact metamorphism that affected both the Upper and the Lower Unit (e.g. Avigad & Garfunkel, 1989; Stolz, Engi & Rickli, 1997; Bröcker & Franz, 1994, 2000).

On Andros, the metamorphic succession can be subdivided into two tectonic units, the Makrotantalon Unit and the Lower Unit of Central-Southern Andros (Papanikoulaou, 1978*a*; Figs A2, A3 in online Appendix at http://journals.cambridge.org/geo). The structurally higher Makrotantalon Unit has a thickness of up to 600 m and mainly consists of clastic metasediments and marbles. Metabasic schists are of subordinate importance. Fossil findings in the dolomitic carbonates yielded Permian ages (Papanikolaou, 1978*a*). The tectonic boundary with the Lower Unit is roughly marked by serpentinites. Judging from structural and geochronological constraints, the Makrotantalon Unit belongs to the upper group of units of the Attic–Cycladic crystalline belt (e.g. Bröcker & Franz, 2006). The Lower Unit (up to 1200 m in thickness) can be correlated with the Cycladic blueschist sequences and mainly consists of a volcano-sedimentary sequence that comprises marbles, carbonate-rich schists, clastic metasediments and metavolcanic rocks (Papanikolaou, 1978*a*). Mineral assemblages document severe greenschist-facies metamorphism, but relict HP rocks can still be found at many places. Judging from field observations, the marble–schist sequences on Andros either represent the stratigraphic continuation or the lithostratigraphic equivalent to the succession exposed in NW Tinos (Papanikolaou, 1978*a*). Disrupted bodies of ultramafic, meta-gabbroic and meta-acidic rocks (up to several hundred metres in length) were recognized at various lithostratigraphic levels (Papanikolaou, 1978*a*; Mukhin, 1996). Some of the occurrences with meta-acidic rock slabs most likely are not part of a mélange, but instead formed by large-scale boudinage processes that affected structurally coherent volcano-sedimentary successions. Ion probe U–Pb zircon dating of such felsic intercalations yielded Triassic protolith ages (∼ 240–249 Ma; Bröcker & Pidgeon, 2007). For details of the local geology see Papanikolaou (1978*a*,*b*), Mukhin (1996), Bröcker & Franz (2006) and Bröcker & Pidgeon (2007).

On Syros (Figs A1, A3), the largest part of the island belongs to the Cycladic blueschist unit, which occurs in two lithostratigraphic or tectonic subunits: an interlayered marble–schist sequence (up to *c*. 2000 m in thickness) and a meta-ophiolitic HP mélange (up to *c*. 200 m) (Dixon & Ridley, 1987; Bröcker & Enders, 2001). Compared to other Cycladic islands, the series of repeated marble horizons and their total thickness is unusual, which led Dixon & Ridley (1987) to suggest tectonic duplication of an originally thinner sequence. Schumacher *et al*. (2008) reported a Lower Carboniferous origin (330–350 Ma) for marbles that occur in the upper part of the metamorphic succession that is based on unpublished findings of presumed foraminifera fossils. Such apparent protolith ages are not supported by U–Pb data of detrital zircons that indicate Triassic to Cretaceous or younger sedimentation (S. Keay, unpub. Ph.D. thesis, Australian National Univ. Canberra, 1998). The Cycladic blueschist unit is tectonically overlain by two allochthonous units: the amphibolite-facies Vari gneisses and a greenschist-facies mylonite sequence. These units show no indications for HP metamorphism and most likely represent down-faulted tectonic slices of the upper group of units (Ridley, 1984).

On Sifnos (Figs A1, A3), the metamorphic succession (*c*. 2500 m thick) belongs entirely to the Cycladic blueschist unit and can be subdivided into an upper Eclogite-Blueschist and a basal Greenschist Unit (Avigad, 1993; Trotet, Jolivet & Vidal, 2001). The Eclogite-Blueschist Unit comprises well-preserved

https://doi.org/10.1017/S001675681100001X Published online by Cambridge University Press

HP rocks intercalated between marble sequences (e.g. Avigad *et al*. 1992; Trotet, Jolivet & Vidal, 2001). A felsic metatuffaceous layer from the basal part of the Eclogite-Blueschist Unit yielded two Triassic age groups of 226.6 ± 2.0 Ma and 240.4 ± 2.1 Ma (Bröcker & Pidgeon, 2007), constraining a maximum depositional age. The Greenschist Unit (*c*. 1000 m thick) is separated by a low-angle normal fault from the overlying sequences and mainly consists of strongly overprinted clastic metasediments, metabasic rocks and marbles (e.g. Avigad *et al*. 1992). HP relics are widespread. The thickness of the inferred crustal interval removed from between both units is controversial (Avigad, 1993; Wijbrans, Schliestedt & York, 1990).

On Naxos (Fig. A2), two tectonic units can be distinguished. The Upper Unit mainly consists of non-metamorphosed sediments (e.g. Gautier, Brun & Jolivet, 1993). The Lower Unit is built up by a migmatite core and a lower grade marble–schist sequence. The migmatite core includes Mesozoic sediments, S-type granites and Variscan orthogneisses. U–Pb zircon dating constrains the time of partial melting to between 20.7 and 16.8 Ma (Keay, Lister & Buick, 2001). The marble–schist series has experienced Tertiary polymetamorphism of eclogite to blueschist grade overprinted by greenschist- to amphibolite-facies conditions and documents a zonal pattern of increasing metamorphic grade (from ∼ 380 °C to ∼ 700 °C) towards the centre of the migmatite dome (e.g. Buick & Holland, 1989; Keay, Lister & Buick, 2001). For meta-bauxite lenses within some marble horizons, Feenstra (1985, 1996) suggested a correlation with non-metamorphic Jurassic bauxites in mainland Greece and the Balkan region, based on geochemical similarities. In the western part of the island, the Lower Unit is bordered by a post-metamorphic granodiorite, which intruded around 12 Ma (Keay, Lister & Buick, 2001).

4. Samples

The calcite marbles are fine- to medium-grained rocks that occur in medium- to thick-bedded sequences of variable thickness (< 1 m to several tens of metres) and lateral extent. Individual occurrences are often disrupted by large-scale boudinage. At the outcrop- or hand specimen scale, the calcite marbles show all colour gradations between white and dark grey, often in alternating layers. Other colour varieties are absent. The mineral assemblage mostly consists of calcite, but dolomite is present in some samples. As accessory phases, phengite, quartz, albite, chlorite and graphite may occur. If present, phengite is often enriched on bedding surfaces. Both hetero- and homeoblastic textures are common. Adjacent domains with widely differing crystal sizes may have different isotopic compositions that can affect the results and interpretations. However, rejection of such material would have completely excluded distinct marble horizons. Highly strained textures are rare. Locally the marbles are isoclinally folded. The m1 marbles are always intercalated with millimetre to decimetre thick quartzite layers (Avigad & Garfunkel, 1989; Bröcker & Franz, 2005). From Tinos, we selected samples that represent the three major marble horizons m3, m2 and m1, and the fossil-bearing lowermost dolomite. From Andros, we chose the m4 and m1 calcite marbles that occur in the upper and lower part of the Lower Unit. The focus on these occurrences ensures complete vertical coverage of the litho- or tectonostratigraphic succession. On Sifnos, we concentrated on marbles from the basal part of the Eclogite-Blueschist Unit that occur above and below the metatuffaceous horizon dated by Bröcker & Pidgeon (2007). The sample location is at Agios Ekaterini near Kamares (Fig. A1). On Syros, we collected samples from a large operating quarry located near Kini, and marbles from the Kampos area (Fig. A1) which show distinct textures resembling pseudomorphs after metamorphic aragonite (Brady *et al*. 2004). On Naxos, we focused on marbles that occur closely associated with meta-bauxite lenses. Samples were collected along the road-cut from Koronas to Lionas and near the emery mines that are located NW of Moutsana (Fig. A2).

The dolomites from the Panormos area on Tinos (> 100 m in thickness) are poorly bedded massive rocks. Their colour is less white than the calcite marbles and shows a weak yellowish tint. Locally a breccia structure is developed, but its origin is unclear. Melidonis (1980) reported well-preserved Triassic (Norian–Rhaetian) fossils (calcareous algae: *Heteroporella*, *Garwoodia*, *Cayeuxia*, *Halimeda*, *Solenopora* and corals: *Thecosmilia clathrata*). Dolomite-rich marbles of the Makrotantalon Unit occur in at least two stratigraphic horizons (*c*. 5–30 m and *c*. 2–20 m thick) with numerous fossiliferous outcrops (calcareous algae, foraminifera and corals) that document Early and Middle to Upper Permian ages, respectively (Papanikolaou, 1978*a*,*b*).

In order to avoid complexities caused by diffusional exchange (e.g. Baker *et al*. 1989; Ganor, Matthews & Paldor, 1989, 1991; Ganor, Matthews & Schliestedt, 1994; Bickle *et al*. 1995), our sampling strategy aimed to obtain samples collected at least 0.5–1 m away from contacts with schists. In several cases, however, the outcrop situation either did not allow us to determine the distance to the next lithological contact, or required sampling at a closer distance to the contact. In order to ensure representative regional coverage as well as complete coverage across the metamorphic succession, such samples were not a priori excluded from further consideration.

From a total of *c*. 150 samples, 75 samples were selected for geochemical studies after petrographic screening under the microscope. Sample selection is based on the assumption that the isotope compositions of bulk samples provide a fit-for-purpose approximation to the original signatures. The presence of dolomite and calcite was determined by staining thin-sections with Alizarin Red-S (Friedman, 1959) and X-ray diffraction of powdered rock material. The main emphasis during final sample selection was to obtain mica-

https://doi.org/10.1017/S001675681100001X Published online by Cambridge University Press

free or mica-poor samples that would be most suitable for Sr-isotope chemostratigraphy. From an early stage on, this approach excluded a relatively large number of marble outcrops, causing a significant disadvantage for regional correlations. In order to assess the isotope geochemical characteristics of 'less-suitable' marbles we have also studied some mica-rich samples from Tinos and Sifnos, but in this case concentrated on calcite mineral separates. Sample locations are shown in Figures A1, A2 and Table A1 in the online Appendix at http://journals.cambridge.org/geo. Petrographic information is summarized in Table A2, and pictures of typical hand specimens and thin-sections are depicted in Figures A4–A13 in the online Appendix.

5. Analytical methods

Samples containing very low modal amounts of white mica were studied as whole rocks. For sample preparation, a *c*. 1 cm thick and 2 × 5 cm rectangular rock slice was cleaned with de-ionized water in an ultrasonic bath and rinsed in ultrapure ethanol. The clean material was crushed in a steel mortar and pulverized in an agate mill. Pre-leaching that is widely used in sample preparation of non-metamorphic carbonates to remove late calcite and/or other contaminants was not performed because all studied samples have experienced diagenesis and complete recrystallization during polyphase metamorphic overprinting. Surface contamination can be ruled out because we studied rock slices with fresh surfaces on all sides that were cut out from the inner part of larger slabs. In the case of higher phengite abundance, the crushed sample was sieved and carbonates were hand-picked from the 180–200 μm grain-size fraction to minimize contamination with micas. Before dissolution, mineral separates were carefully washed in de-ionized water and ultrapure ethanol.

Sr-isotope analyses were carried out at the Institut für Mineralogie, Universität Münster. For this purpose, *c*. 100 mg of whole-rock powder or *c*. 20–50 mg of calcite were dissolved in a H_2O–HCl (2.5 N) mixture on a hot plate overnight. After drying, 2.5 N HCl was added and this mixture was homogenized on a hot plate overnight. After a second evaporation to dryness and centrifugation to remove any residues, Sr was separated by standard ion-exchange procedures (AG 50W-X8 resin) on quartz glass columns using 2.5 N HCl as eluent. For whole-rock samples, a Sr contribution from acid leaching of insoluble impurities (phengite, albite) cannot be completely ruled out, but is considered negligible because, based on thin-section work, samples with considerable amounts of phengite were excluded from further analyses. Consequently, most whole-rock samples display very low Rb concentrations (< 2 ppm) indicating that correction for radiogenic ^{87}Sr is not required. No significant Sr contribution can be expected from albite. Nevertheless, only the lowest values within individual marble groups should be considered as best approximation to the composition of contemporaneous seawater. Mass-spectrometric analysis was carried out using a ThermoFinnigan Triton TIMS for Sr (static mode). Sr was loaded with HCl and TaF_5 on W filaments. Correction for mass fractionation is based on a $^{86}Sr/^{88}Sr$ ratio of 0.1194. Total procedural blanks for Sr were less than 0.1 ng. During two analytical sessions, repeated runs of NBS standard 987 yielded average $^{87}Sr/^{86}Sr$ ratios of 0.710221 ± 0.000034 (2σ, n = 22) and 0.710220 ± 0.000016 (2σ, n = 12), respectively. $^{87}Sr/^{86}Sr$ sample data were normalized to an NBS standard 987 value of 0.710248. The value obtained for the USGS EN-1 standard was 0.709135 ± 0.000016 (2σ, n = 12). Reproducibility was further evaluated by replicate analyses of nine samples.

C- and O-isotope measurements were carried out at the Institut für Geologie und Paläontologie, Universität Münster, using a GasBench connected to a ThermoFinnigan Delta plus XL mass spectrometer via a ConFlo III interface. For individual runs, a sample weight of *c*. 30 μg was used. Results are reported in the standard delta notation as per mil difference relative to V-PDB (Vienna Pee Dee Belemnite). Accuracy was checked against standards IAEA-CO-1 and IAEA-CO-8. Reproducibility, as determined through replicate measurements, was better than ± 0.2 ‰.

Major and trace elements were analysed by Actlabs, Ancaster, Ontario, with ICP-MS methods (Code 4B analytical package). Rb concentrations were determined with X-ray fluorescence spectrometry in pressed pellets (Code 4C1 analytical package). Detection limits for Fe_2O_3, MnO, Sr and Rb are 0.01 wt %, 0.001 wt %, 0.2 ppm and 2 ppm, respectively.

6. Results

6.a. Bulk rock composition and isotope characteristics (Sr, O, C) of mica-poor marbles

6.a.1. Bulk rock compositions

Geochemical data (Table A3 in online Appendix at http://journals.cambridge.org/geo) indicate that the calcite marbles are relatively pure rocks with minor terrigenous contamination. M2 and m3 marbles from Tinos have MgO concentrations that are mostly < 1.0 wt % (Mg/Ca < 0.02), whereas m1 marbles from this island are characterized by more variable MgO contents (< 0.1–6.7 wt %; Mg/Ca up to 0.12), owing to different abundances of dolomite. K_2O and Al_2O_3 concentrations are mostly low (< 0.15 wt % and < 0.1 wt %, respectively). SiO_2 concentrations are more variable (mostly < 0.2 wt %) with a maximum of 1.54 wt % in the Tinos m1 marbles. Rb concentrations are very low (< 2–6 ppm). Sr concentrations range from 86 to 418 ppm, with most samples between 150 and 250 ppm. Bulk compositions of calcite marbles from Andros, Syros, the lower horizon on Sifnos and Naxos show mostly similar ranges (MgO mostly < 1.0 wt %, K_2O < 0.1 wt %, Al_2O_3 < 0.26 wt %, Rb < 2–4 ppm, Sr 90–353 ppm). However, samples from Naxos are characterized by more variable SiO_2 and Rb contents (0.1–1.45 wt % and < 2–36 ppm, respectively) and

https://doi.org/10.1017/S001675681100001X Published online by Cambridge University Press

significantly higher Sr concentrations than observed in samples from other islands (up to ~ 4650 ppm) (Table A3). Dolomitic marbles from Tinos display Mg/Ca ratios between 0.37 and 0.60. Concentrations of SiO_2 (0.07–0.43 wt %, mostly < 0.2 wt %), Al_2O_3 (mostly < 0.03 wt %) and K_2O (< 0.1 wt %) are low, and Sr, Rb and Mn concentrations vary from 44 to 113 ppm, < 2 to 6 ppm and 15 to 77 ppm, respectively. Marbles from the Makrotantalon Unit on Andros are characterized by a broader range in MgO concentrations (1.15–21.02 wt %) indicating variable modal abundance of dolomite (Table A3).

6.a.2. Sr-isotope ratios

With the exception of two data points, the $^{87}Sr/^{86}Sr$ isotope ratios of all samples fall within the range between 0.70698 and 0.70800. On Tinos, the most radiogenic Sr signatures are recorded by m1 marbles from Kalloni (0.70773–0.70861) and the dolomite marbles from the Panormos area (0.70759–0.70792), which can both be distinguished from the Panormos m1 marble (0.70742–0.70756). The Tinos m2 and m3 calcite marbles occurring at higher lithostratigraphic levels are less radiogenic (0.70720–0.70734 and 0.70709–0.70739, respectively). Despite some overlap, there is a clear trend of decreasing $^{87}Sr/^{86}Sr$ values from the m1 marbles towards samples collected from the m2 and m3 horizons (Fig. 2; Table 1). A similar trend has not been observed on Andros where both the lowermost m1 and the topmost m4 marble, which bracket the entire metamorphic succession, show very similar $^{87}Sr/^{86}Sr$ values (0.70709–0.70718; Fig. 2; Table 1). Here, no suitable m2 and m3 marbles are available, as they are all mica-rich and/or strongly weathered. The Sr-isotope data for fossil-bearing and dolomite-rich samples from the Makrotantalon Unit show considerable scatter between 0.70699 and 0.70913. Two calcite marbles from this unit yielded $^{87}Sr/^{86}Sr$ ratios similar to those of m1 and m4 marbles from the Lower Unit. Sr-isotope ratios for the m3 marble on Tinos closely correspond to the Sr-isotope data for the m1 and m4 marbles from Andros, and marbles occurring on top of the radiometrically dated greenschist-gneiss sequence from Sifnos. Samples from two different occurrences on Syros show distinct Sr-isotope characteristics. Marbles from the Kini quarry show values between 0.70756 and 0.70762, whereas Sr-isotope ratios of marbles from Kampos are between 0.70729 and 0.70741. Sr ratios of marbles from Naxos are similar to those from Syros and vary between 0.70737 and 0.70761 (Fig. 2; Table 1).

6.a.3. O- and C-isotope values

Marbles from Tinos display the highest variability in $\delta^{18}O$ with values between −15.5 ‰ and +0.2 ‰ (Tables 1, 2). Despite considerable overlap for some occurrences, $\delta^{18}O$ values allow several subgroups to be distinguished (Figs 3, 4). Most samples, however, including all Tinos m3 and one m2 marbles, the

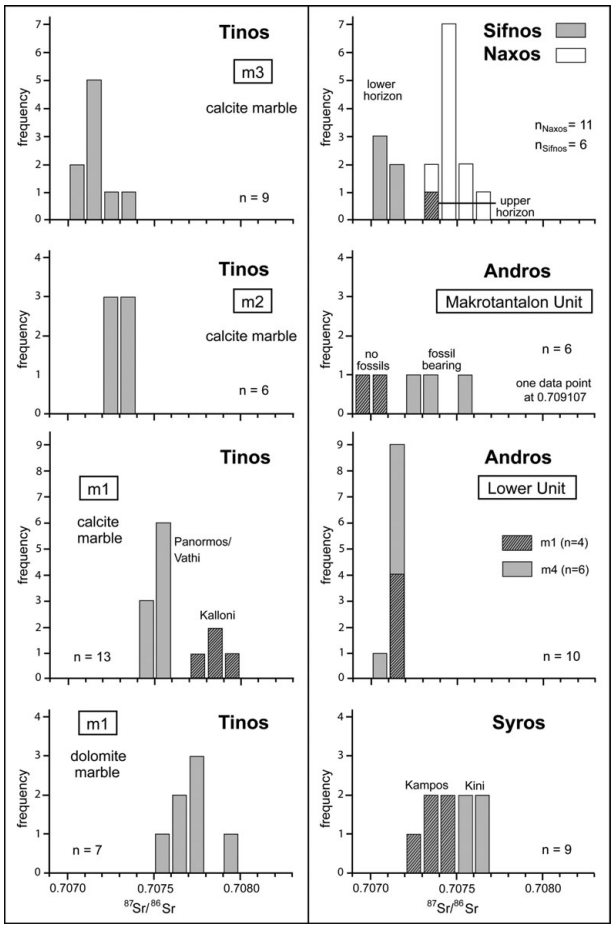

Figure 2. Histograms showing $^{87}Sr/^{86}Sr$ values of 'best quality' (= mica-free or mica-poor) samples, representing various marble units of the Cycladic blueschist belt. For a colour version of this figure see online Appendix at http://journals.cambridge.org/geo.

Andros m1 and m4 marbles, all samples from Sifnos and Syros, and 10 of 11 samples from Naxos, fall within a relatively narrow $\delta^{18}O$ range of −4.8 ‰ to −1.4 ‰. Most of the Tinos m2 marbles and all samples from the Makrotantalon Unit yielded $\delta^{18}O$ values varying between −7.6 ‰ and −5.3 ‰ and between −11.2 ‰ and −5.9 ‰, respectively (Fig. 4; Tables 1, 2). $\delta^{13}C$ values of most samples overlap and fall within the range of 1.0–3.2 ‰ (Fig. 3; Tables 1, 2). Exceptions are the higher $\delta^{13}C$ values of the fossil-bearing samples from the Makrotantalon Unit (1427, 1429, 1443: 3.5 to 5.3 ‰) and the relatively low values (< 1 ‰ to −3.5 ‰) for many samples from Naxos.

6.b. Sr-, C- and O-isotope characteristics of calcite from mica-rich marbles

The Sr-isotope characteristics of mica-rich m3 marbles from Tinos (Table 3) are broadly within the range observed for mica-poor samples (Table 1), but a trend towards higher values is obvious. In the case of the Tinos m2 marbles, six out of eight mica-rich samples are characterized by considerably higher $^{87}Sr/^{86}Sr$ values than mica-poor m2 samples. Mica-rich

https://doi.org/10.1017/S001675681100001X Published online by Cambridge University Press

Table 1. Selected element ratios and $^{87}Sr/^{86}Sr$-, $\delta^{18}O$- and $\delta^{13}C$-values for marbles from Tinos

marble horizon	sample	Mg/Ca	Mn/Sr	Ca/Sr	Sr/Ca	Fe/Sr	$\delta^{18}O$	$\delta^{13}C$	$^{87}Sr/^{86}Sr$ measured	error (2σ)	$^{87}Sr/^{86}Sr$ normalized
m1	T40	0.036	1.33	1791.4	0.55822	1.00	−0.43	2.51	0.707526	0.000010	0.707553
calcite marble	T41	0.050	0.82	988.4	1.01178	0.74	−0.18	2.64	0.707535	0.000011	0.707562
	T43	0.029	0.23	1105.8	0.90429	0.20	−0.56	2.56	0.707467	0.000013	0.707494
	T45	0.118	0.99	1175.1	0.85100	0.48	−0.11	2.97	0.707544	0.000013	0.707571
	T46	0.039	0.78	1176.9	0.84966	0.44	0.18	2.72	0.707480	0.000011	0.707507
	T47	0.036	0.48	1174.5	0.85143	0.44	−0.02	2.82	0.707485	0.000012	0.707511
	T57	0.042	0.27	2293.4	0.43604	0.88	−1.42	2.04	0.707471	0.000015	0.707497
	T58	0.049	0.35	2233.8	0.44767	0.88	−1.05	2.16	0.707393	0.000011	0.707420
	T67	0.018	0.84	1337.9	0.74742	0.24	−0.85	2.97	0.707510	0.000016	0.707537
	5212	0.004	2.06	2251.0	0.44425	2.83	−9.02	2.49	0.707819	0.000014	0.707846
	5213	0.010	5.28	2932.3	0.34103	6.36	−9.83	2.74	0.707707	0.000013	0.707734
	5214	0.011	4.60	2814.1	0.35535	5.58	−9.31	2.80	0.707779	0.000015	0.707805
	5215	0.003	0.77	1660.0	0.60242	0.87	−15.47	2.57	0.708584	0.000015	0.708611
	5216	0.001	1.00	2887.5	0.34632	1.01	−12.22	2.68	0.707923	0.000013	0.707950
m1	T51	0.604	0.35	4943.5	0.20229	2.27	−1.51	2.54	0.707737	0.000009	0.707764
dolomite marble	T52	0.433	0.45	6872.7	0.14550	2.27	−1.27	2.33	0.707659	0.000017	0.707686
	T55	0.391	0.48	3804.8	0.26282	2.41	−0.92	2.18	0.707640	0.000012	0.707667
	T56	0.445	0.75	5741.5	0.17417	1.89	−0.51	2.19	0.707568	0.000016	0.707594
	T60	0.372	0.36	2914.3	0.34314	0.89	−1.39	2.08	0.707732	0.000012	0.707758
	T61	0.387	0.36	2973.6	0.33629	1.82	−1.84	2.12	0.707739	0.000014	0.707766
	1423	0.520	0.69	2084.3	0.47978	5.57	−0.80	2.15	0.707889	0.000014	0.707915
m2	T10	0.011	0.22	937.3	1.06693	3.68	−3.13	2.92	0.707313	0.000012	0.707340
	T11	0.009	0.30	2576.9	0.38806	1.78	−5.73	2.96	0.707313	0.000010	0.707339
	T12	0.008	0.72	4736.8	0.21111	1.63	−5.25	1.45	0.707175	0.000013	0.707202
	T13	0.002	0.25	3195.7	0.31292	2.27	−5.38	1.81	0.707235	0.000009	0.707261
	T23	0.009	0.33	2860.7	0.34957	0.49	−5.27	2.72	0.707276	0.000016	0.707303
	T24	0.015	0.59	3036.3	0.32935	1.59	−7.63	2.34	0.707223	0.000014	0.707250
m3	T20	0.031	0.20	2586.0	0.38670	2.30	−3.50	2.19	0.707084	0.000013	0.707111
	T32	0.007	0.11	3178.3	0.31464	1.14	−3.34	2.14	0.707075	0.000012	0.707101
	T33	0.005	0.13	3600.6	0.27773	0.65	−3.30	2.54	0.707117	0.000012	0.707143
	T34	0.007	0.13	3587.2	0.27877	2.68	−2.97	1.92	0.707229	0.000014	0.707256
	T35	0.007	0.11	2744.2	0.36440	1.47	−4.51	2.26	0.707066	0.000012	0.707093
	T36	0.007	0.11	2785.7	0.35898	1.49	−4.24	2.13	0.707128	0.000011	0.707155
	T37	0.008	0.10	2550.4	0.39210	0.90	−3.09	2.33	0.707071	0.000010	0.707097
	T38	0.008	0.10	2585.3	0.38680	1.82	−1.48	2.30	0.707105	0.000016	0.707132
	T65	0.007	0.04	2412.3	0.41454	0.44	−3.06	2.75	0.707362	0.000018	0.707388

marbles from the upper horizon of the Kamares area on Sifnos show values between 0.70730 and 0.70742, and can clearly be distinguished from the mica-poor lower horizon (0.70708–0.70713) of this location. O- and C-isotope values of mica-rich samples from Tinos (Table 3) are within the same range as the mica-poor samples (Table 1). A difference between both groups exists for samples from Sifnos (Tables 2, 3). Here, $\delta^{13}C$ values from mica-poor samples are less positive than mica-rich samples. The $\delta^{18}O$ range of marbles from Sifnos, however, is comparable.

7. Discussion

7.a. Is it possible to use the Sr-, O- and C-isotope ratios of Cycladic marbles for regional correlations?

Owing to their distinct mineralogical composition and colour, marbles are used on some islands to subdivide monotonous schist sequences. However, the lack of distinctive petrographic characteristics (e.g. colour, principal components, characteristic accessory phases, depositional textures) prevents utilization of the metamorphic carbonates for island-to-island correlations. The present study aimed to identify distinctive Sr-, O- and C-isotope characteristics for specific marble horizons that would allow establishment of improved regional correlations and lithostratigraphic subdivision within the study area. For this objective, all samples including the mica-rich marbles were taken into consideration. For general geochemical fingerprinting across the study area, even severely altered marbles have the potential to serve as valuable marker horizons. We focused on systematic sampling of marbles from Tinos and Andros, and studied to a lesser extent marbles from Syros, Sifnos and Naxos. In the case of Naxos, previous studies documented the potential of marble O- and C-isotope data for archaeological fingerprinting (e.g. Herz, 1987, 1992; Cramer, 1998 and references therein). For Syros and Sifnos, the database is yet too small to fully determine its significance for this purpose.

On a local scale, Sr-, O- and C-isotope characteristics allow discrimination of some occurrences from the total marble population. Based on their $^{87}Sr/^{86}Sr$ values, the upper and lower horizon exposed in the Kamares area on Sifnos can clearly be distinguished. The Naxos samples show similarities to marbles from Syros, but are clearly separated from marbles occurring on Tinos (m3), Andros (m4–m1) and Sifnos (upper Kamares horizon) (Fig. 2). The combination of Sr- and O-isotope signatures also allows distinguishing between some marble occurrences on Tinos and Andros (Fig. 4).

https://doi.org/10.1017/S001675681100001X Published online by Cambridge University Press

Table 2. Selected element ratios and $^{87}Sr/^{86}Sr$-, $\delta^{18}O$- and $\delta^{13}C$-values for marbles from Andros, Syros and Sifnos

marble horizon	sample	Mg/Ca	Mn/Sr	Ca/Sr	Sr/Ca	Fe/Sr	$\delta^{18}O$	$\delta^{13}C$	$^{87}Sr/^{86}Sr$ measured	error (2σ)	$^{87}Sr/^{86}Sr$ normalized
Andros, Makrotantalon Unit	A 90	0.020	0.09	1138.1	0.00088	2.71	−6.07	4.71	0.706990	0.000013	0.707016
	A 91	0.018	0.07	876.7	0.00114	1.95	−5.86	5.25	0.706960	0.000014	0.706986
	1427	0.144	0.15	805.0	0.00124	1.21	−11.17	2.80	0.707270	0.000019	0.707297
	1428	0.122	0.11	757.5	0.00132	2.70	−11.12	3.52	0.707284	0.000012	0.707310
	1429	0.282	0.19	574.2	0.00174	0.86	−11.12	2.61	0.707509	0.000014	0.707535
	1443	0.583	5.25	2500.1	0.00040	44.22	−6.56	3.78	0.709107	0.000027	0.709134
Andros, Lower Unit m1	A 96	0.009	0.22	1396.4	0.00072	1.49	−2.29	2.99	0.707139	0.000013	0.707166
	A 98	0.007	0.77	1672.7	0.00060	2.11	−2.95	2.52	0.707150	0.000010	0.707176
	A 100	0.009	0.24	1208.5	0.00083	3.89	−2.84	3.13	0.707106	0.000012	0.707132
	A 102	0.009	0.31	1282.6	0.00078	2.11	−2.59	2.99	0.707118	0.000012	0.707145
Andros, LU m2	5561	0.011	0.14	1186.0	0.00084	0.64	−5.50	2.21	0.707106	0.000008	0.707134
Andros, LU m3	5571	0.002	0.11	1384.0	0.00072	6.45	−7.01	2.71	0.707207	0.000007	0.707235
Andros, Lower Unit m4	A 92	0.008	0.63	1182.4	0.00085	2.33	−4.47	2.22	0.707107	0.000013	0.707134
	A 93	0.011	0.59	1207.3	0.00083	0.21	−3.28	2.29	0.707075	0.000013	0.707102
	A 95	0.008	0.55	1095.9	0.00091	0.79	−3.96	2.21	0.707063	0.000020	0.707089
	5565	0.009	0.51	1181.4	0.00085	1.90	−4.69	2.27	0.707082	0.000008	0.707110
	5566	0.012	0.63	1122.5	0.00089	0.81	−3.77	2.21	0.707085	0.000008	0.707113
	5567A	0.013	0.68	1119.1	0.00089	3.09	−3.73	2.22	0.707131	0.000008	0.707159
Syros, Kampos	SY 106	0.005	0.15	1922.2	0.00052	1.33	−3.15	2.55	0.707388	0.000011	0.707414
	SY 107	0.005	0.06	1670.3	0.00060	1.16	−2.60	2.94	0.707296	0.000013	0.707322
	SY 109	0.006	0.13	1339.8	0.00075	2.56	−3.06	2.56	0.707375	0.000011	0.707402
	SY 111	0.005	0.11	2786.7	0.00036	1.94	−1.62	2.92	0.707271	0.000015	0.707298
	SY 112	0.004	0.06	1466.6	0.00068	0.50	−2.88	2.79	0.707346	0.000013	0.707372
Syros, Kini	SY 114	0.013	0.13	3271.5	0.00031	–	−1.76	1.19	0.707551	0.000010	0.707578
	SY 115	0.011	0.43	2717.7	0.00037	7.83	−1.41	1.51	0.707539	0.000016	0.707565
	5256	0.027	0.12	2918.8	0.00034	–	−2.26	2.27	0.707587	0.000015	0.707613
	5257	0.009	0.24	2533.3	0.00039	3.96	−3.43	1.91	0.707596	0.000013	0.707623
Sifnos, upper horizon	5289	0.016	0.09	2206.5	0.00045	–	−2.79	2.54	0.707342	0.000016	0.707369
Sifnos, lower horizon	5294	0.011	0.21	2596.0	0.00039	0.93	−3.03	2.28	0.707048	0.000014	0.707075
	5295	0.010	0.20	2541.7	0.00039	1.36	−4.75	2.42	0.707102	0.000014	0.707128
	5296	0.013	0.40	2531.2	0.00040	9.60	−3.83	2.48	0.707053	0.000014	0.707080
	5297	0.009	0.43	2706.4	0.00037	7.72	−3.79	2.31	0.707069	0.000014	0.707095
	5298	0.010	0.32	2748.7	0.00036	2.45	−1.86	2.32	0.707075	0.000012	0.707102
Naxos meta-bauxite	5401	0.003	0.17	4440.7	0.00023	0.78	−4.27	1.50	0.707455	0.000010	0.707483
	5402	0.006	0.25	3173.6	0.00032	2.78	−2.93	2.15	0.707462	0.000008	0.707490
	5403	0.668	0.14	2032.4	0.00049	1.25	−2.13	2.02	0.707584	0.000007	0.707612
	5404	0.012	2.42	2225.9	0.00045	11.72	−3.00	−3.53	0.707523	0.000007	0.707551
	5405	0.004	0.16	4160.7	0.00024	1.44	−3.45	0.43	0.707540	0.000007	0.707568
	5406	0.007	0.06	1511.4	0.00066	1.85	−5.29	−0.37	0.707393	0.000009	0.707421
	5407	0.011	0.00	84.6	0.01182	0.23	−2.74	−0.32	0.707386	0.000008	0.707414
	5408	0.014	0.01	220.2	0.00454	0.23	−3.51	0.78	0.707380	0.000008	0.707408
	5409	0.010	0.03	375.8	0.00266	0.72	−3.93	−1.14	0.707407	0.000008	0.707435
	5410B	0.010	0.02	604.2	0.00166	0.11	−3.89	−1.50	0.707380	0.000008	0.707408
	5411	0.014	0.01	226.0	0.00443	0.04	−2.57	0.21	0.707339	0.000008	0.707367

On the other hand, many marbles show significant overlap of Sr-, O- and C-isotope ratios, which either documents primary compositional characteristics or the influence of various post-depositional alteration processes. For example, the $^{87}Sr/^{86}Sr$ ratios for marbles from Andros (m4 and m1), Tinos (m3) and Sifnos (upper marble horizon) are almost identical. This may indicate simultaneous carbonate precipitation in an area of larger extent and would justify a correlation of these occurrences. In this case, identical Sr-isotope values of marbles representing the lowest and highest parts of the metamorphic succession on Andros would be in accordance with models either suggesting isoclinal folding/thrusting of a single horizon, or very fast sedimentation. However, owing to repeated oscillations of the seawater curve in the most likely Mesozoic–Cenozoic interval of sediment formation, identical Sr-isotope values may also record different protolith ages, possibly implying non-existing temporal and spatial relationships for distinct marble horizons. At this point, we cannot prove or disprove which of these alternatives are correct. With the available information at hand, it cannot be assessed to what extent original Sr signals are preserved. The interpretation of O- and C-isotope data faces similar problems.

The present study complements existing data sets for identification of archaeological provenance of Aegean marbles (e.g. Lazzarini & Antonelli, 2003; Capedri, Venturelli & Photiades, 2004; Brilli, Cavazzini & Turi, 2005; Zöldföldi & Satir, 2003), but the suitability of Sr-, O- and C-isotope ratios for correlating marble horizons occurring on different Cycladic islands cannot be demonstrated. The Sr-, O- and C-isotope ratios, alone or in various combinations, are not diagnostic enough to unravel mutual relationships between individual marble occurrences.

https://doi.org/10.1017/S001675681100001X Published online by Cambridge University Press

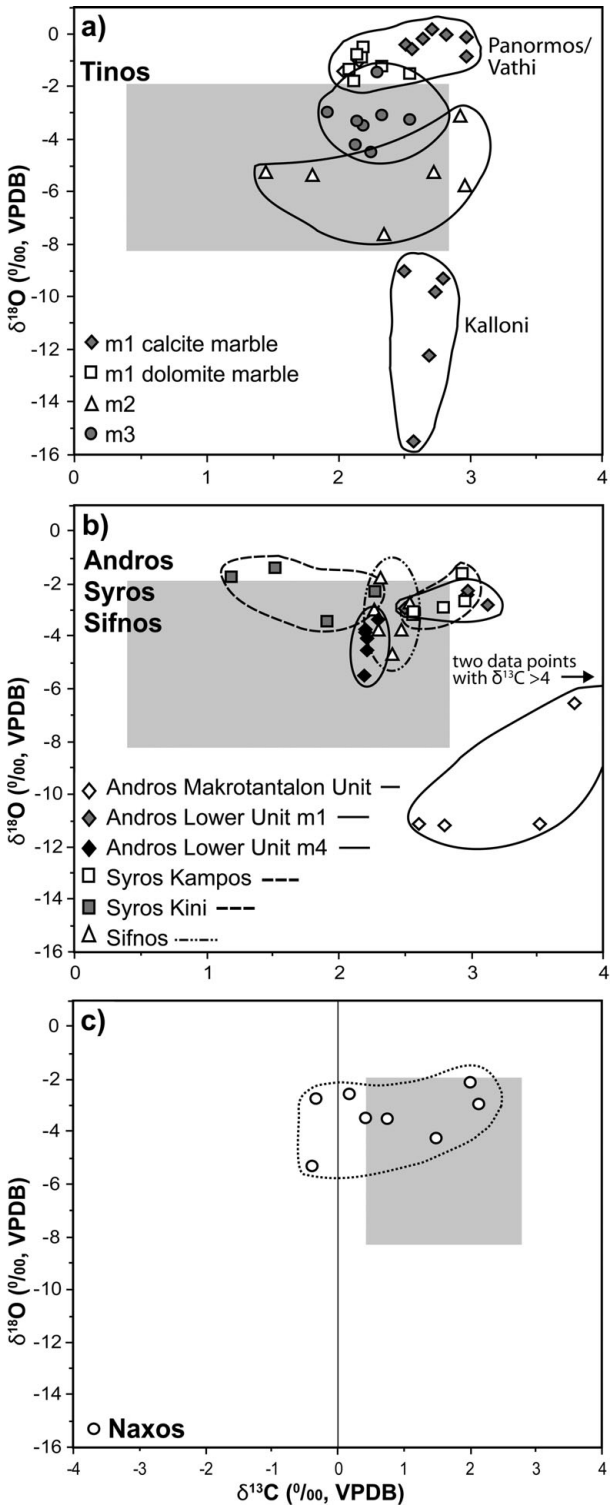

Figure 3. $\delta^{18}O$ v. $\delta^{13}C$ diagram showing isotope data of 'best quality' (= mica-free or mica-poor) marbles from the Cycladic blueschist belt. Grey field outlines oxygen- and carbon-isotope compositions of marbles from the western Cyclades (Ganor, Matthews & Schliestedt, 1994) that were collected more than 1 m away from a contact with schists.

7.b. Sr-isotope chemostratigraphy: criteria for sample selection

In principle, Sr-isotope chemostratigraphy can provide a depositional age of marine carbonates, if their $^{87}Sr/^{86}Sr$ ratios have not been altered substantially through post-depositional processes. These include diagenesis (compaction, cementation, dissolution, recrystallization, replacement of aragonite by calcite, interaction with meteoric waters, e.g. Scholle & Ulmer-Scholle, 2003) as well as alteration during metamorphic overprinting (e.g. recrystallization, diffusional exchange, deformation, interaction with metamorphic fluids). In addition, modifications of the $^{87}Sr/^{86}Sr$ values can result from contamination with terrigenous components. Individually or combined, all these processes can have a considerable effect on the apparent age derived from the $^{87}Sr/^{86}Sr$ ratio. Hence, a rigorous sample screening is necessary in order to identify the least altered rocks. In order to select the most promising samples, we applied a combination of petrographic criteria (rejection of domains with microveins, only mica-free or mica-poor marbles) and geochemical parameters (Figs 5, 6) with the main emphasis on Mn/Sr, $\delta^{18}O$ and $\delta^{13}C$ values.

Increased Mn concentrations are considered to represent a sensitive indicator of meteoric diagenetic processes, and the Mn/Sr ratio is often taken as a parameter to identify the least altered samples, although different threshold values have been proposed (e.g. Kaufman & Knoll, 1995; Thomas *et al*. 2004 and references therein). In this study, we follow Thomas *et al*. (2004) and consider samples with Mn/Sr values < 0.6 as suitable for Sr-isotope chemostratigraphy. Some studies suggested that $\delta^{18}O$ isotope values < -6 ‰ also indicate that samples are too altered for Sr-isotope stratigraphy (Kaufman & Knoll, 1995; Fölling & Frimmel, 2002). O- and C-isotope studies of Cycladic marbles showed that $\delta^{18}O$ and $\delta^{13}C$ values of marbles collected away from contacts with schists record the isotopic composition of marine carbonates (e.g. Ganor, Matthews & Paldor, 1989, 1991). For marbles from Tinos, Sifnos and Kithnos that were collected at least 1 m away from a lithological contact, Ganor, Matthews & Schliestedt (1994) reported O-isotope values of -1.95 ‰ to -8.25 ‰ (recalculated to V-PDB from SMOW (Standard Mean Ocean Water) values of 22.4 ‰ to 28.9 ‰, respectively) and $\delta^{13}C$ values of 0.4 ‰ to 2.8 ‰ (Fig. 3) with the alteration trend directed towards more negative $\delta^{18}O$ and $\delta^{13}C$ values. Similar isotope characteristics were reported by Baker *et al*. (1989) for unaltered marbles from Naxos. The most recent isotope study from Naxos documented an accumulation of $\delta^{18}O$ and $\delta^{13}C$ data points for marbles that were collected > 1 m from lithological contacts at -2 ‰ to -9 ‰ and 0 to 4 ‰, respectively (Ebert *et al*. 2010). Ganor, Matthews & Schliestedt (1994) also showed that very low $\delta^{13}C$ values (-2.2 ‰ to -11.5 ‰) are diagnostic for samples containing late calcite overgrowths or veins.

Using the Mn/Sr criterion, the degree of preservation of primary $^{87}Sr/^{86}Sr$ signatures is highly variable (see Table 1). On Tinos, all m1 samples from the Kalloni location, half of the m1 sample population from Panormos and two out of six samples representing the m2 marble horizon are considered to be too altered

https://doi.org/10.1017/S001675681100001X Published online by Cambridge University Press

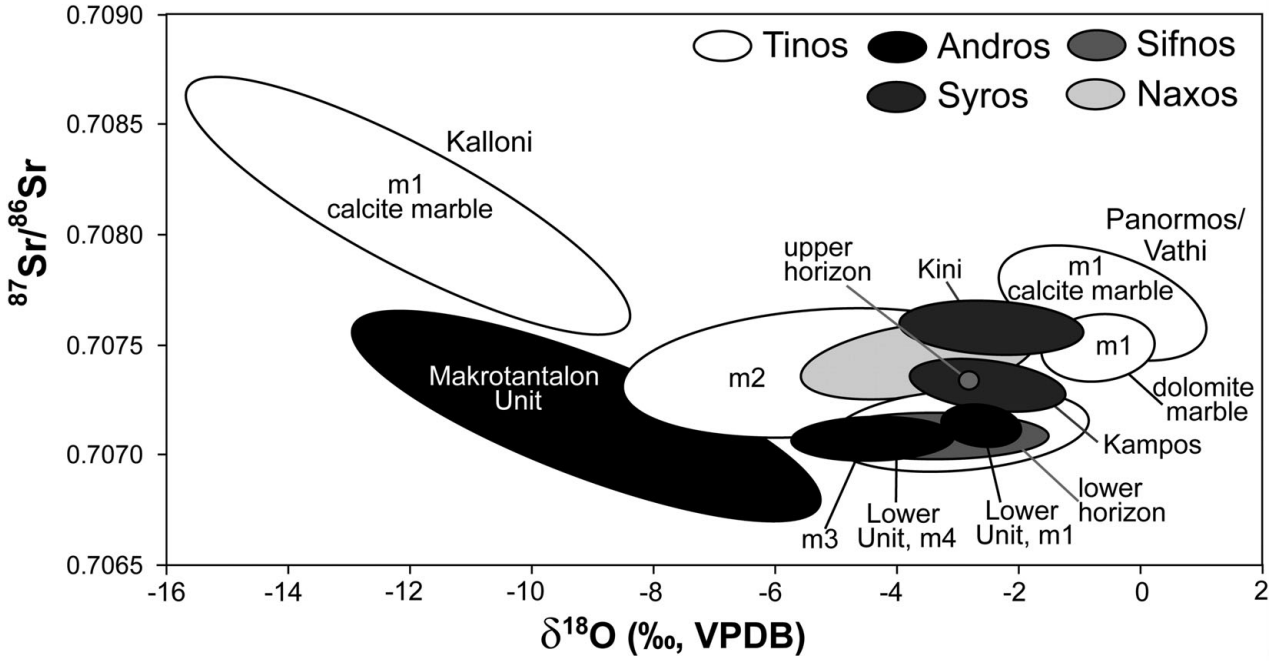

Figure 4. $^{87}Sr/^{86}Sr$ v. $\delta^{18}O$ diagram showing isotope data of 'best quality' (= mica-free or mica-poor) marbles from the Cycladic blueschist belt. For a colour version of this figure see online Appendix at http://journals.cambridge.org/geo.

for Sr chemostratigraphy. The lowest Mn/Sr ratios (< 0.2) were recognized in samples collected from the m3 marble horizon. Five out of seven dolomites from the Panormos area are characterized by Mn/Sr < 0.6. With few exceptions, the new O- and C-isotope results (Tables 1, 2) are within the compositional ranges observed for marbles that are unaffected by diffusional exchange (e.g. Ganor, Matthews & Schliestedt, 1994; Ebert *et al*. 2010). Based on $\delta^{18}O$ and $\delta^{13}C$ values, the marbles from Tinos can be separated into four groups (Fig. 3a), mostly according to the different marble horizons. $\delta^{18}O$ values corroborate that m1 marbles from Kalloni are too altered for Sr-isotope stratigraphy. Most samples from the m2 horizon and all m3 samples appear to be suited for Sr chemostratigraphy, using the Mn/Sr–$\delta^{18}O$ data. This also pertains to m1 calcite marbles from Panormos and m1 dolomite marbles (Fig. 6e). Most marbles from Andros, Syros, Sifnos and Naxos show no correlation between the Mn/Sr ratios and $\delta^{18}O$ isotope values (Fig. 6f) and plot within the compositional ranges for non-altered marbles. Three samples from Naxos were excluded from further consideration because of $\delta^{13}C$ values < −1 ‰ and/or Mn/Sr > 0.6. Five out of six samples from the Makrotantalon Unit on Andros are characterized by favourable Mn/Sr ratios. However, $\delta^{18}O$ and/or $\delta^{13}C$ suggest alteration. Nevertheless, we accepted the two apparently least altered samples

Table 3. $^{87}Sr/^{86}Sr$-, $\delta^{18}O$- and $\delta^{13}C$-values for mica-rich marbles from Tinos and Sifnos

marble horizon	sample	$\delta^{18}O$	$\delta^{13}C$	$^{87}Sr/^{86}Sr$ measured	error (2σ)	$^{87}Sr/^{86}Sr$ normalized
Tinos, m2	T1	−1.53	2.14	0.707634	0.000008	0.707662
	T2	−3.57	3.17	0.707654	0.000008	0.707682
	T3	−1.20	2.22	0.707635	0.000007	0.707663
	T4	−1.51	2.20	0.707719	0.000008	0.707647
	5206	−11.25	3.34	0.707689	0.000007	0.707717
	5209	−2.44	2.03	0.707878	0.000008	0.707906
	5229	−3.18	2.89	0.707299	0.000008	0.707327
	5230	−3.11	2.74	0.707309	0.000008	0.707337
Tinos, m3	T21	−2.18	1.98	0.707024	0.000008	0.707052
	T22	−4.08	1.82	0.707106	0.000008	0.707134
	T72	−3.66	2.39	0.707353	0.000009	0.707381
	T73	−2.49	2.51	0.707343	0.000008	0.707371
	T74	−3.08	3.65	0.707416	0.000009	0.707444
	T75	−2.53	2.07	0.707223	0.000007	0.707251
Sifnos, upper horizon	5288	−3.25	2.89	0.707376	0.000007	0.707404
	5290	−3.62	3.00	0.707304	0.000008	0.707332
	5291	−2.12	2.96	0.707396	0.000007	0.707424
	5292	−2.87	3.01	0.707317	0.000009	0.707345
	5293	−2.95	2.94	0.707273	0.000008	0.707301

https://doi.org/10.1017/S001675681100001X Published online by Cambridge University Press

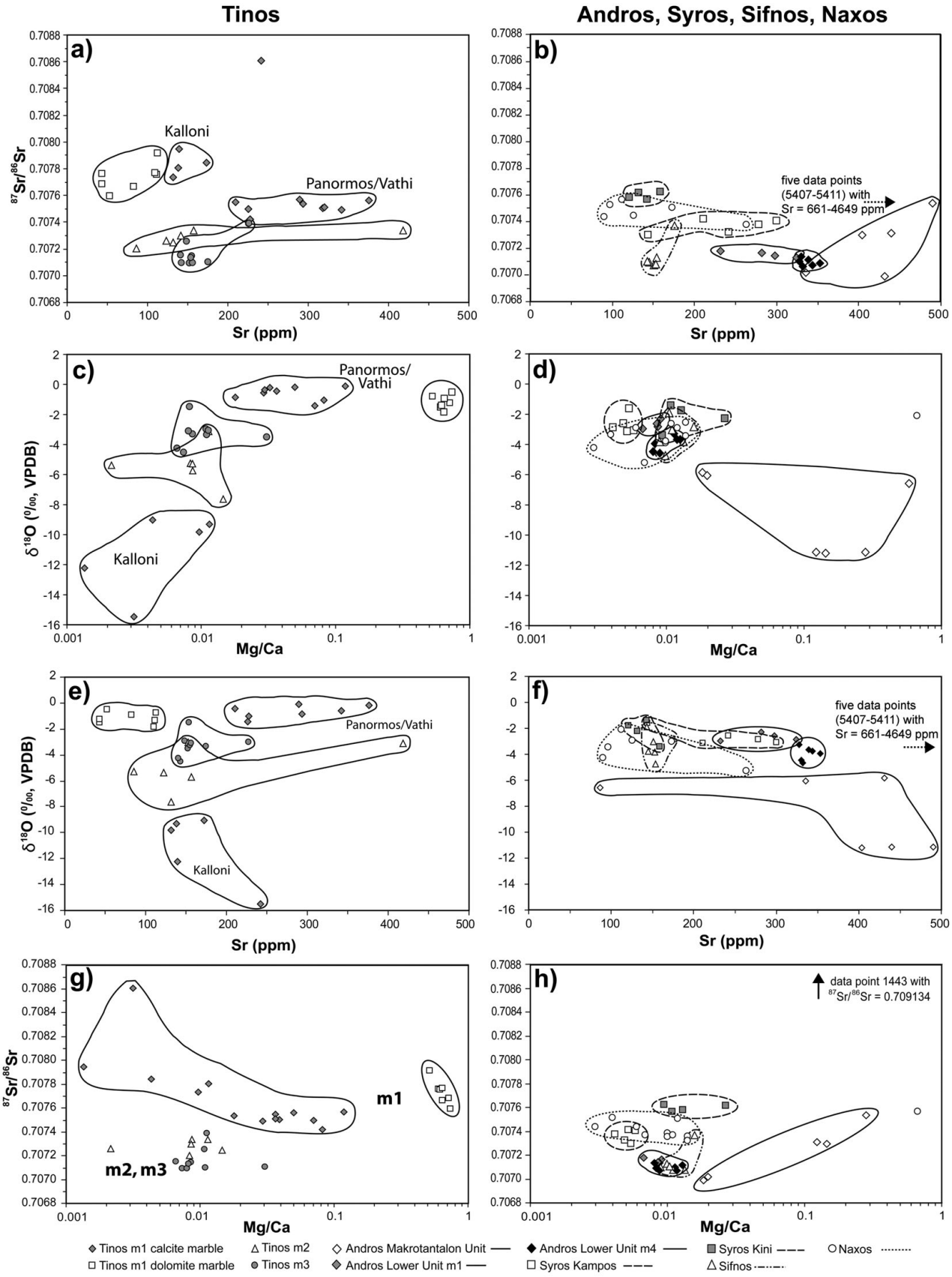

Figure 5. Selected geochemical parameters for 'best quality' (= mica-free or mica-poor) marbles from the Cycladic blueschist belt. Left-hand column – Tinos; right-hand column – Andros, Syros, Sifnos, Naxos. For a colour version of this figure see online Appendix at http://journals.cambridge.org/geo.

https://doi.org/10.1017/S001675681100001X Published online by Cambridge University Press

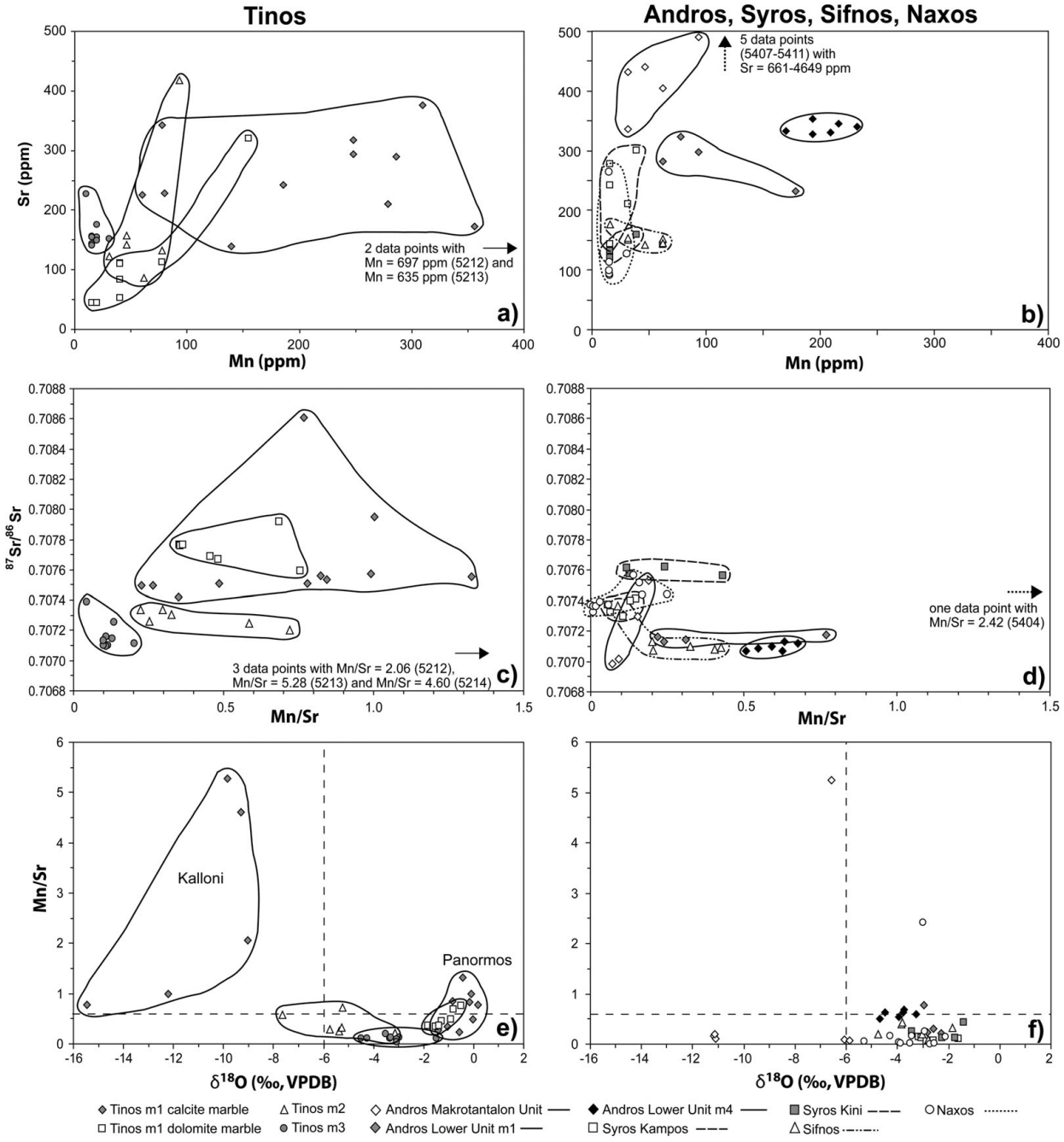

Figure 6. Sr v. Mn, $^{87}Sr/^{86}Sr$ v. Mn/Sr and Mn/Sr v. $\delta^{18}O$ diagrams for 'best quality' (= mica-free or mica-poor) marbles from the Cycladic blueschist belt. Left-hand column – Tinos; right-hand column – Andros, Syros, Sifnos, Naxos. Dashed lines indicate the screening parameters Mn/Sr = 0.6 and $\delta^{18}O = -6$ ‰. For a colour version of this figure see online Appendix at http://journals.cambridge.org/geo.

($\delta^{13}C$ = 4.71 and 5.25), because biostratigraphic control is available.

Most of the studied marbles are characterized by relatively low Sr concentrations that possibly indicate considerable Sr loss during the aragonite–calcite transformation. Although the Mn/Sr ratios often are in accordance with low degrees of alteration, and would even be more favourable in the case of higher Sr contents, a high degree of uncertainty remains over what extent the primary Sr-isotope signal is still preserved.

7.c. Is it possible to extract ages from the screened data set?

The $^{87}Sr/^{86}Sr$ values for the least altered samples intersect the seawater curve multiple times within the likely time interval of original carbonate precipitation (< 240 Ma; as indicated by SHRIMP U–Pb zircon data; e.g. Bröcker & Pidgeon, 2007). Thus, an unequivocal age assignment is not possible. At least in the present example, Sr-isotope chemostratigraphy requires bracketing age constraints from radiometric dating and/or biostratigraphy. Such well-defined chronometric fixed points are avail-

https://doi.org/10.1017/S001675681100001X Published online by Cambridge University Press

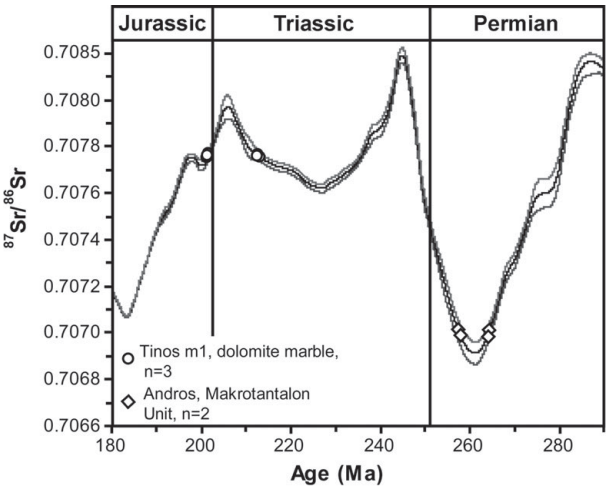

Figure 7. Apparent depositional ages for marbles from fossil-bearing horizons from Tinos and Andros as indicated by the marine Sr-isotope curve of McArthur *et al*. (2001, LOWESS table 4b database), showing all possible intersections for the most likely time interval of deposition. Tinos – shown are data points with Mn/Sr < 0.6, $\delta^{18}O > -6$ ‰ and $\delta^{13}C$ between 0 ‰ and 3.0 ‰. Andros – shown are data points with $\delta^{18}O < -6.07$ ‰ and $\delta^{13}C$ of 4.71–5.25 ‰.

able for some parts of the studied metamorphic successions.

7.c.1. Tinos

There is general consensus that a tectonic contact separates the m1 calcite marbles from a lower fossil-bearing dolomite sequence; however, the nature of this fault zone is unclear and has either been related to thrusting or extensional processes (Avigad & Garfunkel, 1989; Bröcker & Franz, 2005). Matthews *et al*. (1999) showed that the fault zone and adjacent rock volumes are characterized by lowered C- and O-isotope values, which were explained by focused fluid infiltration of externally derived low $\delta^{18}O$–$\delta^{13}C$ fluids along the tectonic contact. It is not clear whether or not this process has also influenced the Sr-isotope values. Nevertheless, the m1 calcite marbles and the dolomites have Sr-isotope signatures that roughly correspond to the Rhaetian–Norian fossil record of the dolomites (Melidonis, 1980; Fig. 7), suggesting an age of 190–215 Ma for carbonate formation. The $^{87}Sr/^{86}Sr$ data would be in accordance with an interpretation that suggests a relatively small age difference between the rock sequences occurring on both sides of the fault zone. Least altered m2 and m3 marbles that occur at higher lithostratigraphic levels show a relatively small range in $^{87}Sr/^{86}Sr$ (0.70709–0.70739) that can be projected onto various Jurassic and Cretaceous limbs of the oscillating seawater curve (Fig. 8a, b). The distinct Sr-isotope values for samples collected at different levels of the lithostratigraphic succession suggest that these layers represent a temporal succession and not the tectonic repetition of a single horizon. If we accept this interpretation, the m2 marble should be older than the m3 horizon. This would encourage an interpretation that postulates a *c*. 185–190 Ma age

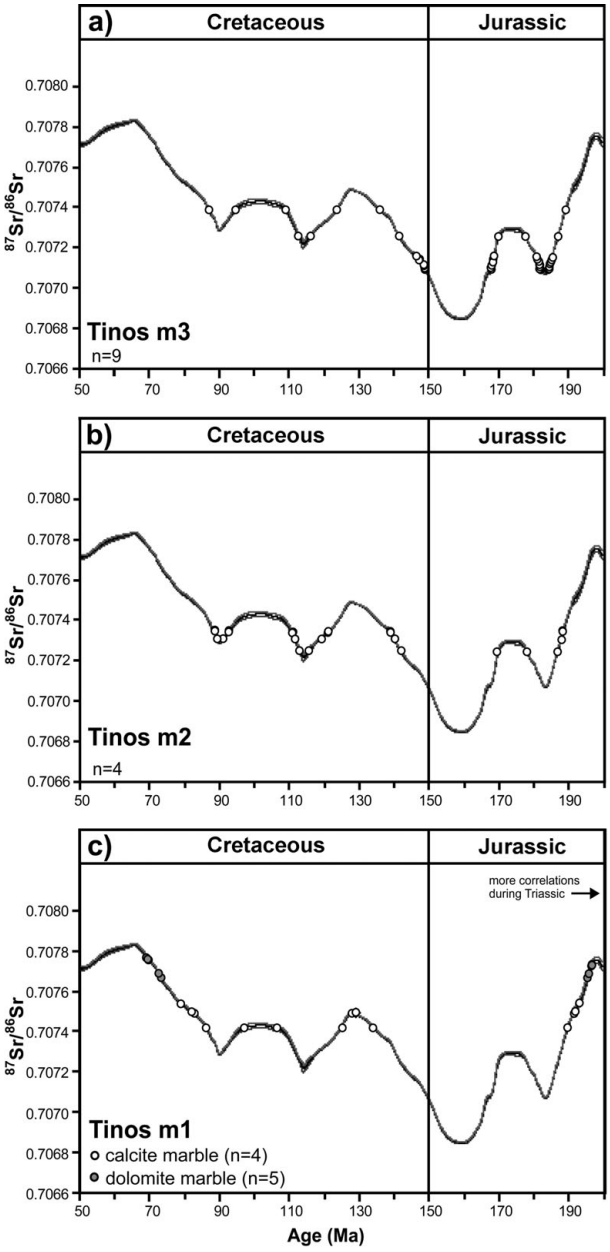

Figure 8. Apparent depositional ages for marbles from Tinos, as indicated by the marine Sr-isotope curve of McArthur *et al*. (2001, LOWESS table 4b database), showing all possible intersections for the most likely time interval of deposition. Shown are data points with Mn/Sr < 0.6, $\delta^{18}O > -6$ ‰ and $\delta^{13}C$ between 0 ‰ and 3.0 ‰.

for the m2 marbles, but still leaving several Jurassic and Cretaceous intercept options for the m3 marbles (Fig. 8a, b). In the case that the interpretation of 80 Ma old zircons in clastic metasediments as detrital phases is correct (Bulle *et al*. 2010), most $^{87}Sr/^{86}Sr$ values for the m3 marbles would suggest an age that is older than predicted by the U–Pb data.

7.c.2. Andros

The fossil-bearing dolomitic marbles from Andros show a large variability in $^{87}Sr/^{86}Sr$, suggesting disturbance of the original signal. However, two out of six Sr values would still conform to the biostratigraphically assigned Permian age (Papanikolaou, 1978*a*,*b*; Fig.

https://doi.org/10.1017/S001675681100001X Published online by Cambridge University Press

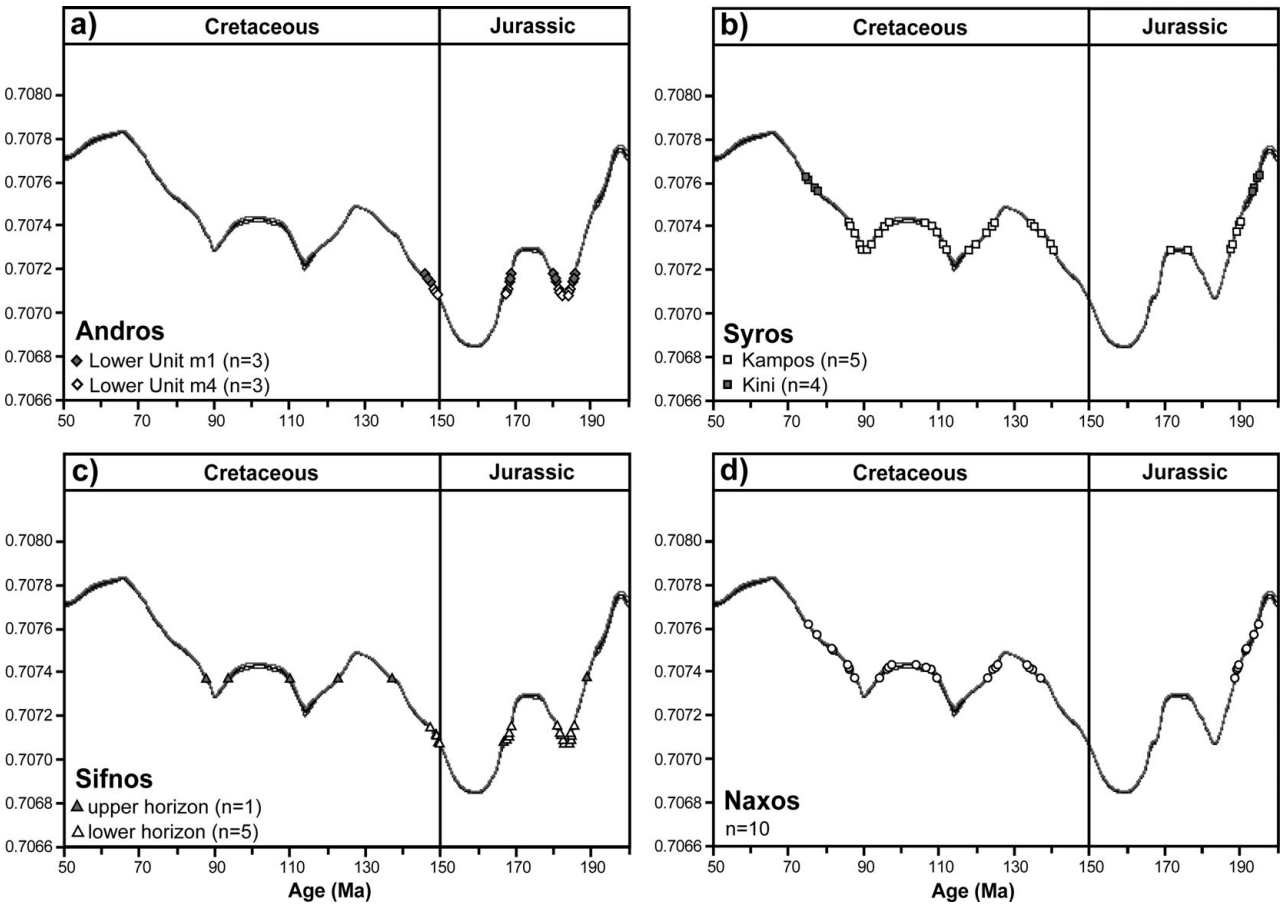

Figure 9. Apparent depositional ages for marbles from Andros, Syros, Sifnos and Naxos, as indicated by the marine Sr-isotope curve of McArthur *et al*. (2001, LOWESS table 4b database), showing all possible intersections for the most likely time interval of deposition. Shown are data points with Mn/Sr < 0.6, $\delta^{18}O > -6$ ‰ and $\delta^{13}C$ between −0.4 ‰ and 3.1 ‰.

7). The meta-acidic rocks from the Lower Unit, collected between m4 and m1, most likely represent boudinaged meta-volcanic intercalations that provide a Triassic reference point for sediment formation (~240–249 Ma; Bröcker & Pidgeon, 2007). However, caution is warranted in interpreting these U–Pb ages as robust time markers. A proximal meta-igneous source may yield a sediment that largely mimics the bulk compositional and age characteristics of the source rocks (e.g. S. Keay, unpub. Ph.D. thesis, Australian National Univ. Canberra, 1998). In this case, the zircon ages would only constrain the age of the source rocks, but not the depositional age. The m4 and m1 marbles from Andros yield a tight $^{87}Sr/^{86}Sr$ data cluster. When plotted onto the seawater curve (Fig. 9a), they indicate different Jurassic or Cretaceous ages (*c*. 180–185 Ma, *c*. 168 Ma, *c*. 145–150 Ma) that could only be reconciled with the U–Pb data if the host rocks of the Triassic zircon populations represent recycled material.

7.c.3. Syros

We consider Triassic to Cretaceous U–Pb zircon ages for clastic metasediments (S. Keay, unpub. Ph.D. thesis, Australian National Univ. Canberra, 1998) as a more reliable indicator for the maximum time of sedimentation than a fossil-based Carboniferous age reported by Schumacher *et al*. (2009), which is possibly compromised by bad preservation or reworking. The studied marbles define two distinct groups which are both characterized by higher $^{87}Sr/^{86}Sr$ values than measured for the main Tinos–Andros–Sifnos subgroup (Fig. 9b). Sr-isotope characteristics of marbles from Kini are similar to those of the Panormos m1 marbles, indicating a Jurassic age (*c*. 190 Ma), but would also be consistent with a Cretaceous age of formation (*c*. 75 Ma). Sr-isotope values of marbles from Kampos agree with the seawater curve at an apparent age of *c*. 185–190 Ma and several times between *c*. 85–140 Ma (Fig. 9b). As on Tinos, the youngest age group recorded in clastic metasediments occurs at ~ 75–80 Ma, but was interpreted, like similar ages in metasediments from Ios and Naxos, as evidence for unspecified metamorphic processes (S. Keay, unpub. Ph.D. thesis, Australian National Univ. Canberra, 1998). The next youngest age groups indicate ages of ~ 108 Ma and 135 Ma.

7.c.4. Sifnos

A fossil occurrence (Négris, 1914) and U–Pb zircon data (Bröcker & Pidgeon, 2007) indicate a sedimentation age < 230 Ma. The $^{87}Sr/^{86}Sr$ values of marbles

https://doi.org/10.1017/S001675681100001X Published online by Cambridge University Press

exposed below the meta-tuffaceous Kamares sequence indicate various Jurassic or Cretaceous ages (Fig. 9c), which are in accordance with the independent age constraints.

7.c.5. Naxos

In dolomitic marbles, Dürr & Flügel (1979) recognized remnants of Upper Triassic algae and foraminifers. Detrital zircon populations of various types of metasediments suggest that the maximum depositional ages are younger than Late Triassic–Jurassic (S. Keay, unpub. Ph.D. thesis, Australian National Univ. Canberra, 1998). The Sr-isotope values of marbles from Naxos intersect the seawater curve at *c*. 185–195 Ma and multiple times between *c*. 140 and *c*. 75 Ma (Fig. 9d).

7.c.6. Summary

Only in rare and exceptional circumstances may Sr-isotope chemostratigraphy of metamorphic rocks yield geologically meaningful age information. The preservation of original isotopic signatures is possible, but even in such cases, only very broad time constraints can be deduced if well-defined chronometric fixed points are available. More subtle distinctions are not feasible. The complexities in assessing the degree of alteration as well as the fact that many of the independent age constraints are also not free of ambiguity make it yet impossible to use the Sr-isotope data of the Cycladic marbles for age determination.

8. Conclusions

This study clearly shows the limitations of Sr-, O- and C-isotope ratios in marble as a tool for unravelling the litho- and/or tectonostratigraphic relationships across the Attic–Cycladic crystalline belt that are thus far obscured by the fragmentary outcrop pattern. These isotope ratios, alone or in various combinations, are not diagnostic enough to unravel mutual relationships between individual marble occurrences. Both matching as well as different isotope data may reflect primary compositional characteristics or superimposed effects of various post-depositional alteration processes. In most cases, an unambiguous interpretation is impossible.

The time of sediment deposition of the Cycladic marbles could not be determined based on the Sr-isotope data. Even in the case that the initial marine Sr-isotope ratio is preserved, the Sr signal alone is not sufficient to identify the age of pre-metamorphic carbonate formation. Oscillations of the Sr-isotope seawater curve in the most likely time interval of biogenic precipitation (Triassic–Cretaceous time), and the scarcity of independent time markers prevent a rigid chemostratigraphic interpretation. The Sr-isotope data cannot unambiguously be linked to specific segments of the seawater curve.

The Sr-, O- and C-isotope values of the Aegean marbles will remain of interest for archaeological provenance studies, but are unsuitable to resolve lithostratigraphic relationships on and between different islands. U–Pb dating of zircon-bearing metavolcanic rocks can assist solving litho- or tectonostratigraphic relationships, but suitable rocks of this kind are thinly distributed over the study area. More promising are the widespread siliciclastic metasediments and the age and provenance information that can be deduced from their detrital zircon populations. A detailed zircon database that documents contrasts and/or similarities in sedimentation history and provenance can provide the foundation for further correlations and subdivisions on individual islands and across the region.

Acknowledgements. This study was funded by the Deutsche Forschungsgemeinschaft (grant BR 1068/12–1). Thanks are due to H. Baier and A. Fugmann for laboratory assistance and support on the mass spectrometers. Thorough reviews by two anonymous reviewers helped considerably to improve the manuscript.

References

ALTHERR, R., KREUZER, H., WENDT, I., LENZ, H., WAGNER, G. A., KELLER, J., HARRE, W. & HÖHNDORF, A. 1982. A Late Oligocene/Early Miocene high temperature belt in the Attic-Cycladic Crystalline Complex (SE Pelagonian, Greece). *Geologisches Jahrbuch* **E23**, 97–164.

ALTHERR, R., SCHLIESTEDT, M., OKRUSCH, M., SEIDEL, E., KREUZER, H., HARRE, W., LENZ, H., WENDT, I. & WAGNER, G. A. 1979. Geochronology of high-pressure-rocks on Sifnos (Cyclades, Greece). *Contributions to Mineralogy and Petrology* **70**, 245–55.

ALTHERR, R. & SIEBEL, W. 2002. I-type plutonism in a continental back-arc setting: Miocene granitoids from the central Aegean Sea, Greece. *Contributions to Mineralogy and Petrology* **134**, 397–415

AVIGAD, D. 1993. Tectonic juxtaposition of blueschists and greenschists in Sifnos Island (Aegean Sea) – implications for the structure of the Cycladic blueschist belt. *Journal of Structural Geology* **15**, 1459–469.

AVIGAD, D. & GARFUNKEL, Z. 1989. Low-angle faults above and below a blueschist belt-Tinos Island, Cyclades, Greece. *Terra Nova* **1**, 182–87.

AVIGAD, D., GARFUNKEL, Z., JOLIVET, L. & AZANON, J. M. 1997. Back arc extension and denudation of Mediterranean eclogites. *Tectonics* **16**, 924–41.

AVIGAD, D., MATTHEWS, A., EVANS, B. W. & GARFUNKEL, Z. 1992. Cooling during exhumation of a blueschist terrane: Sifnos (Cyclades, Greece). *European Journal of Mineralogy* **4**, 619–34.

BAKER, J., BICKLE, M. J., BUICK, I. S., HOLLAND, T. J. B. & MATTHEWS, A. 1989. Isotopic and petrological evidence for the infiltration of a water-rich fluid during the Miocene M2 metamorphism on Naxos, Greece. *Geochimica et Cosmochimica Acta* **53**, 2037–50.

BANNER, J. L. 2004. Radiogenic isotopes: systematics and applications to earth surface processes and chemical stratigraphy. *Earth Science Reviews* **65**, 141–94.

BICKLE, M. J., CHAPMAN, H. J., WICKHAM, S. M. & PETERS, M. T. 1995. Strontium and oxygen isotope profiles across marble-silicate contacts, Lizzies Basin, East Humboldt Range, Nevada: constraints on metamorphic permeability contrasts and fluid flow. *Contributions to Mineralogy and Petrology* **121**, 400–13.

BRADY, J. B., MARKLEY, M. J., SCHUMACHER, J. C., CHENEY, J. T. & BIANCIARDI, G. R. 2004. Aragonite pseudomorphs in high-pressure marbles of Syros, Greece. *Journal of Structural Geology* **26**, 3–9.

BRILLI, M., CAVAZZINI, G. & TURI, B. 2005. New data of $^{87}Sr/^{86}Sr$ ratio in classical marble: an initial database for marble provenance determination. *Journal of Archaeological Science* **32**, 1543–551.

BRÖCKER, M., BIEHLING, D., HACKER, B. & GANS, P. 2004. High-Si phengite records the time of greenschist facies overprinting: implications for models suggesting megadetachments in the Aegean Sea. *Journal of Metamorphic Geology* **22**, 427–42.

BRÖCKER, M. & ENDERS, M. 1999. U-Pb zircon geochronology of unusual eclogite-facies rocks from Syros and Tinos (Cyclades, Greece). *Geological Magazine* **136**, 111–118.

BRÖCKER, M. & ENDERS, M. 2001. Unusual bulk-rock compositions in eclogite facies rocks from Syros and Tinos (Cyclades, Greece): implications for U-Pb zircon geochronology. *Chemical Geology* **175**, 581–603.

BRÖCKER, M. & FRANZ, L. 1994. The contact aureole on Tinos (Cyclades, Greece). Part I: Field relationships, petrography and P-T conditions. *Chemie der Erde* **54**, 262–80.

BRÖCKER, M. & FRANZ, L. 1998. Rb-Sr isotope on Tinos Island (Cyclades, Greece): additional time constraints for metamorphism, extent of infiltration-controlled overprinting and deformational activity. *Geological Magazine* **135**, 369–82.

BRÖCKER, M. & FRANZ, L. 2000. Contact metamorphism on Tinos (Cyclades, Greece): the importance of tourmaline, timing of the thermal overprint and Sr isotope characteristics. *Mineralogy and Petrology* **70**, 257–83.

BRÖCKER, M. & FRANZ, L. 2005. The base of the Cycladic blueschist unit on Tinos island (Greece) re-visited: field relationships, phengite-geochemistry and Rb-Sr-geochronology. *Neues Jahrbuch für Mineralogie – Abhandlungen* **181**, 81–93.

BRÖCKER, M. & FRANZ, L. 2006. Dating metamorphism and tectonic juxtaposition on Andros Island (Cyclades): results of a Rb-Sr-study. *Geological Magazine* **143**, 609–20.

BRÖCKER, M. & KEASLING, A. 2006. Ionprobe U-Pb-zircon ages from the high-pressure/low-temperature mélange of Syros, Greece: age diversity and the importance of pre-Eocene subduction. *Journal of Metamorphic Geology* **24**, 615–31.

BRÖCKER, M., KREUZER, H., MATTHEWS, A. & OKRUSCH, M. 1993. $^{40}Ar/^{39}Ar$ and oxygen isotope studies of polymetamorphism from Tinos Island, Cycladic blueschist belt. *Journal of Metamorphic Geology* **11**, 223–40.

BRÖCKER, M. & PIDGEON, R. T. 2007. Protolith ages of metaigneous and metatuffaceous rocks from the Cycladic blueschist unit, Greece: results of a reconnaissance U-Pb Zircon study. *Journal of Geology* **115**, 83–98.

BUICK, I. S. & HOLLAND, T. J. B. 1989. The P-T-t path associated with crustal extension, Naxos, Cyclades, Greece. In *Evolution of Metamorphic Belts*. (eds J. S. Daly, R. A. Cliff & B. W. S. Yardley), pp. 365–69. Geological Society of London, Special Publication no. 43.

BULLE, F., BRÖCKER, M., GÄRTNER, C. & KEASLING, A. 2010. Geochemistry and geochronology of HP mélanges from Tinos and Andros, Cycladic blueschist belt, Greece. *Lithos* **117**, 61–81.

CAPEDRI, S., VENTURELLI, G. & PHOTIADES, A. 2004. Accessory minerals and $\delta^{18}O$ and $\delta^{13}C$ of marbles from the Mediterranean area. *Journal of Cultural Heritage* **5**, 27–47.

CRAMER, T. 1998. Die Marmore des Telephosfrieses am Pergamonaltar. *Berliner Beiträge zur Archäometrie* **15**, 95–198.

DIXON, J. E. & RIDLEY, J. R. 1987. Syros. In *Chemical Transport in Metasomatic Processes* (ed. H. C. Helgeson), pp. 489–501. Dordrecht: Reidel Publishing Company.

DÜRR, S., ALTHERR, R., KELLER, J., OKRUSCH, M. & SEIDEL, E. 1978. The Median Aegean Crystalline Belt: stratigraphy, structure, metamorphism, magmatism. In *Alps, Apennines, Hellenides* (eds H. Closs, D. H. Roeder & K. Schmidt), pp. 455–477. IUGS report no. 38, Schweizerbart, Stuttgart.

DÜRR, S. & FLÜGEL, H. 1979. Contribution à la stratigraphie du cristallin des Cyclades: mise en évidence du Trias supérieur dans les marbres de Naxos (Grèce). *Rapport de la Commission Internationale de la Mer Méditerranée* **25/26 (2a)**, 31–2.

EBERT, A., GNOS, E., RAMSEYER, K., SPANDLER, C., FLEITMANN, D., BITZIOS, D. & DECROUEZ, D. 2010. Provenance of marbles from Naxos based on microstructural and geochemical characterization. *Archaeometry* **52**, 209–28.

FEENSTRA, A. 1985. Metamorphism of bauxites on Naxos, Greece. Ph.D. Thesis, University of Utrecht. *Geologica Ultraiectina* **39**, 1–206.

FEENSTRA, A. 1996. An EMP and TEM-AEM study of margarite, muscovite and paragonite in polymetamorphic metabauxites of Naxos (Cyclades, Greece) and the implications of fine-scale mica interlayering and multiple mica generations. *Journal of Petrology* **37**, 201–33.

FÖLLING, P. G. & FRIMMEL, H. E. 2002. Chemostratigraphic correlation of carbonate successions in the Gariep and Saldania Belts, Namibia and South Africa. *Basin Research* **13**, 1–37.

FRIEDMAN, G. M. 1959. Identification of carbonate minerals by staining methods. *Journal of Sedimentary Petrology* **29**, 87–97.

GANOR, J., MATTHEWS, A. & PALDOR, N. 1989. Constraints on effective diffusivity during oxygen isotope exchange at a marble ± schist contact, Sifnos (Cyclades) Greece. *Earth Planetary Science Letters* **94**, 208–16.

GANOR, J., MATTHEWS, A. & PALDOR, N. 1991. Diffusional isotopic exchange across an interlayered marble-schist sequence with an application to Tinos, Cyclades, Greece. *Journal of Geophysical Research* **96**, 18073–80.

GANOR, J., MATTHEWS, A. & SCHLIESTEDT, M. 1994. Post metamorphic low δ13C calcite veins in the Cycladic complex (Greece) and their implications for modeling fluid infiltration processes using carbon isotope compositions. *European Journal of Mineralogy* **6**, 365–79.

GAUTIER, P. & BRUN, J. P. 1994. Ductile crust exhumation and extensional detachments in the central Aegean (Cyclades and Evvia Islands). *Geodinamica Acta* **7**, 57–85.

GAUTIER, P., BRUN, J.-P. & JOLIVET, L. 1993. Structure and kinematics of Upper Cenozoic extensional detachment on Naxos and Paros (Cyclades Islands, Greece). *Tectonics* **12**, 1180–94.

HERZ, N. 1987. Carbon and oxygen isotopic ratios: a data base for classical Greek and Roman Marble. *Archaeometry* **29**, 35–43.

HERZ, N. 1992. Provenance determination of neolithic to classical Mediterranean marbles by stable isotopes. *Archaeometry* **34**, 185–94.

JOLIVET, L. & PATRIAT, M. 1999. Ductile extension and the formation of the Aegean Sea. In *The Mediterranean Basins: Tertiary extension within the Alpine Orogen* (eds B. Durand, L. Jolivet, F. Horvath & M. Séranne), pp. 427–56. Geological Society of London, Special Publication no. 156.

JOLIVET, L., FACENNA, C., GOFFÉ, B., BUROV, E. & AGARD, P. 2003. Subduction tectonics and exhumation of high-pressure metamorphic rocks in the Mediterranean orogen. *American Journal of Science* **303**, 353–409.

KATZIR, Y., MATTHEWS, A., GARFUNKEL, Z. & SCHLIESTEDT, M. 1996. The tectono-metamorphic evolution of a dismembered ophiolite (Tinos, Cyclades, Greece). *Geological Magazine* **133**, 237–54.

KAUFMAN, A. J. & KNOLL, A. H. 1995. Neoproterozoic variations in the C-isotopic composition of seawater: stratigraphic and biogeochemical implications. *Precambrian Research* **49**, 301–27.

KEAY, S., LISTER, G. & BUICK, I. 2001. The timing of partial melting, Barrovian metamorphism and granite intrusion in the Naxos metamorphic core complex, Cyclades, Aegean Sea, Greece. *Tectonophysics* **342**, 275–312.

KEITER, M., PIEPJOHN, K., BALLHAUS, C., LAGOS, M. & BODE, M. 2004. Structural development of high-pressure metamorphic rocks on Syros island (Cyclades, Greece). *Journal of Structural Geology* **26**, 1433–45.

KRIJGSMAN, W. 2002. The Mediterranean: Mare Nostrum of Earth Sciences. *Earth and Planetary Science Letters* **205**, 1–12.

LAZZARINI, L. & ANTONELLI, F. 2003. Petrographic and isotopic characterization of the marble of the island of Tinos (Greece). *Archaeometry* **45**, 541–52.

MATTHEWS, A., LIEBERMAN, J., AVIGAD, D. & GARFUNKEL, Z. 1999. Fluid-rock interaction and thermal evolution during thrusting of an Alpine metamorphic complex (Tinos island, Greece). *Contributions to Mineralogy and Petrology* **135**, 212–24.

MATTHEWS, A. & SCHLIESTEDT, M. 1984. Evolution of the blueschist and greenschist facies rocks of Sifnos, Cyclades, Greece. *Contributions to Mineralogy and Petrology* **88**, 150–63.

MCARTHUR, J. M. 1994. Recent trends in strontium isotope stratigraphy. *Terra Nova* **6**, 331–58.

MCARTHUR, J. M., HOWARTH, R. J. & BAILEY, T. R. 2001. Strontium-Isotope-Stratigraphy: LOWESS Version 3. Best-fit line to the marine Sr-Isotope curve for 0–509 Ma accompanying look-up table for deriving numerical age. *Journal of Geology* **109**, 155–69.

MELEZHIK, V. A., GOROKHOV, I. M., FALLICK, A. E. & GJELLE, S. 2001. Strontium and carbon isotope geochemistry applied to dating of carbonate sedimentation: an example from high-grade rocks of the Norwegian Caledonides. *Precambrian Research* **108**, 267–92.

MELEZHIK, V. A, ROBERTS, D., FALLICK, A. E., GOROKHOV, I. M. & KUSNETZOV, A. B. 2005. Geochemical preservation potential of high-grade calcite marble versus dolomite marble: implication for isotope chemostratigraphy. *Chemical Geology* **216**, 203–24.

MELIDONIS, N. G. 1980. The geological structure and mineral deposits of Tinos Island (Cyclades – Greece). In *The Geology of Greece*, vol. **13**, pp.1–80. Athens: Institute of Geological and Mineral Exploration.

MUKHIN, P. 1996. The metamorphosed olistostromes and turbidites of Andros Island, Greece, and their tectonic significance. *Geological Magazine* **133**, 697–711.

NASCIMENTO, R. S. C., SIAL, N. A. & PIMENTEL, M. M. 2007. C- and Sr-isotope systematics applied to Neoproterozoic marbles of the Seridó belt, northeastern Brazil. *Chemical Geology* **237**, 191–210.

NÉGRIS, P H. 1914. *Roches cristallophylliennes et tectonique de la Grèce*, pp. 25–32. Imprimerie P. D. Sakellarios, Athènes.

OKRUSCH, M. & BRÖCKER, M. 1990. Eclogites associated with high-grade blueschists in the Cyclades archipelago, Greece: a review. *European Journal of Mineralogy* **2**, 451–78.

PAPANIKOLAOU, D. J. 1978*a*. Contribution to the geology of Aegean Sea: the island of Andros. *Annales Geologiques des pays Helleniques* **29**, 477–553.

PAPANIKOLAOU, D. 1978*b*. Geological map of Andros, 1:50000. Athens: Publication Department of Geological Maps of I.G.M.E.

PARRA, T., VIDAL, O. & JOLIVET, L. 2002. Relation between the intensity of deformation and retrogression in blueschist metapelites of Tinos Island (Greece) evidenced by chlorite-mica local equilibra. *Lithos* **63**, 41–66.

PATZAK, M., OKRUSCH, M. & KREUZER, H. 1994. The Akrotiri unit on the island of Tinos, Cyclades, Greece: witness to a lost terrane of Late Cretaceous age. *Neues Jahrbuch für Geologie und Paläontologie – Abhandlungen* **194**, 211–52.

RIDLEY, J. 1984. Listric normal faulting and the reconstruction of the synmetamorphic structural pile of the Cyclades. In *The geological evolution of the Eastern Mediterranean* (eds J. E. Dixon & A. H. F. Robertson), pp. 755–61. Geological Society of London, Special Publication no. 17.

SCHOLLE, P. A. & ULMER-SCHOLLE, D. S. 2003. *A Color Guide to the Petrography of Carbonate Rocks: Grains, textures, porosity, diagenesis*. American Association of Petroleum Geologists Memoir 77, Tulsa, 474 pp.

SCHUMACHER, J. C., BRADY, J. B., CHENEY, J. T. & TONNSEN, R. R. 2008. Glaucophane-bearing Marbles on Syros, Greece. *Journal of Petrology* **49**, 1667–86.

STOLZ, J., ENGI, M. & RICKLI, M. 1997. Tectonometamorphic evolution of SE Tinos, Cyclades, Greece. *Schweizerisch Mineralogisch Petrographische Mitteilungen* **77**, 209–31.

THOMAS, C. W., GRAHAM, C. M., ELLAM, R. M. & FALLICK, A. E. 2004. $^{87}Sr/^{86}Sr$ chemostratigraphy of Neoproterozoic Dalradian limestones of Scotland and Ireland: constraints on depositional ages and time scales. *Journal of the Geological Society, London* **161**, 229–42.

TOMASCHEK, F., KENNEDY, A. K., VILLA, I. M., LAGOS, M. & BALLHAUS, C. 2003. Zircons from Syros, Cyclades, Greece – recrystallization and mobilization of zircon during high-pressure metamorphism. *Journal of Petrology* **44**, 1977–2002.

TROTET, F., JOLIVET, L. & VIDAL, O. 2001. Tectono-metamorphic evolution of Syros and Sifnos Islands (Cyclades, Greece). *Tectonophysics* **338**, 179–209.

VAN GELDERN, R., JOACHIMSKI, M. M., DAY, J., JANSEN, U., ALVAREZ, F., YOLKIN, E. A. & MA, X.-P. 2006. Carbon, oxygen and strontium isotope records of Devonian brachiopod shell calcite. *Palaeogeography, Palaeoclimatology, Palaeoecology* **240**, 47–67.

VEIZER, J., ALA, D., AZMY, K., BRUCKSCHEN, P., BUHL, D., BRUHN, F., CARDEN, G. A. F., DIENER, A., EBNETH, S., GODDERIS, Y., JASPER, T., KORTE, C., PAWELLEK, F., PODLAHA, O. G. & STRAUSS, H. 1999. $^{87}Sr/^{86}Sr$, $\delta^{13}C$, $\delta^{18}O$ evolution of Phanerozoic seawater. *Chemical Geology* **161**, 59–88.

https://doi.org/10.1017/S001675681100001X Published online by Cambridge University Press

WIJBRANS, J. R. & MCDOUGALL, I. 1988. Metamorphic evolution of the Attic Cycladic Metamorphic Belt on Naxos (Cyclades, Greece) utilizing $^{40}Ar/^{39}Ar$ age spectrum measurements. *Journal of Metamorphic Geology* **6**, 571–94.

WIJBRANS, J. R., SCHLIESTEDT, M. & YORK, D. 1990. Single grain argon laser probe dating phengites from the blueschist to greenschist transition on Sifnos (Cyclades, Greece). *Contributions to Mineralogy and Petrology* **104**, 582–93.

ZÖLDFÖLDI, J. & SATIR, M. 2003. Provenance of white marble building stones in the monuments of the ancient Troia. In *Troia and the Troad* (eds G. A. Wagner, E. Pernicka & H. P. Uerpmann), pp. 203–223. Berlin: Springer.

https://doi.org/10.1017/S001675681100001X Published online by Cambridge University Press